Ut sementem feceris, ita metes.

Marcus Tullius Cicero

TECHNISCHE UNIVERSITÄT WIEN
Vienna University of Technology

DIPLOMA THESIS

Bioorthogonal bond-cleavage reactions applying self-immolative linkers

conducted at the

Institute of Applied Synthetic Chemistry

of Vienna University of Technology

under supervision of

Univ.Prof. Dipl.-Ing. Dr.techn.Johannes **Fröhlich**,

Univ.Ass. Dipl.-Ing. Dr.techn.Hannes **Mikula**

and

Dipl.-Ing. Dr.techn.Philipp **Skrinjar**, BSc

by

Patrick Keppel

3385 Gerersdorf, Lechnerstraße 3

Vienna, April 23, 2019

Kurzfassung

Im letzten Jahrzehnt haben sich bioorthogonale Bindungsspaltungsreaktionen basierend auf der IEDDA-Reaktion (inverse-electron-demand Diels-Alder) von *trans*-Cyclooctenen und Tetrazinen als vielversprechende Strategie für potentielle *in vivo* Freisetzung von Zielmolekülen etabliert. Seit ihrer Entdeckung wurden zahlreiche Ansätze unternommen, um ihre Leistung im Hinblick auf bioorthogonale Kompatibilität, Reaktionskinetik sowie vollständiger Freisetzung gewünschter Zielmoleküle zu optimieren. Vor kurzem wurde der Umfang der Pyridazin Eliminierung erweitert, um weitere Funktionalitäten neben Carbamaten zu spalten.

Aufgrund dieser Einschränkungen, insbesondere der Freisetzung von Phenolen und primären Aminen, wurde das bekannte Konzept selbstzerstörender Linker (SIL) als ermutigender Ansatz eingeführt, um die Kinetik der Pyridazin Eliminierung zu verbessern. Zwei verschiedene selbstzerstörende Linker für die Freisetzung von Phenolen bzw. primären Aminen wurden erfolgreich eingeführt, welche beide zu einer Freisetzung bei stark beschleunigter Kinetik führten.

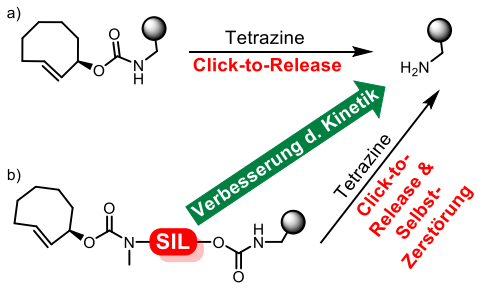

Abbildung 1. Gegenüberstellung der etablierten Click-to-Release Strategie (a) und der erweiterten Strategie für Click-to-Release Experimente mit selbstzerstörenden Linkern (b).

Erstmals konnte im Vergleich zu Literaturreferenzen nahezu vollständige Freisetzung primärer Amine erreicht werden. Darüber hinaus konnte die pH-Abhängigkeit (pH 4-9) hinsichtlich der Geschwindigkeit freigesetzter Verbindungen aufgeklärt und deren Optimum ermittelt werden. Die pH-Abhängigkeit der Kinetik von Click-to-Release und Selbstzerstörung betonte erneut die Wichtigkeit des Reaktionsumfeldes auf die gesamte Abbaukette.

Abstract

In the last decade bioorthogonal bond-cleavage reactions based on the IEDDA (inverse-electron-demand Diels-Alder) reaction of *trans*-cyclooctenes and tetrazines have emerged as a promising strategy for potential *in vivo* release of target molecules. Since their discovery, numerous approaches have been investigated to optimize their performance in terms of bioorthogonal compatibility, kinetics and complete release of desired target compounds. Recently, the scope of pyridazine elimination has been extended in order to cleave further moieties besides carbamates.

Suffering from the limitations mentioned, with regard for the release of phenols and primary amines, the known concept of self-immolative linkers (SIL) was introduced as an encouraging approach to enhance pyridazine elimination kinetics. Two different self-immolative linkers for the release of phenols respectively primary amines were sufficiently introduced that both led to release at highly accelerated kinetics.

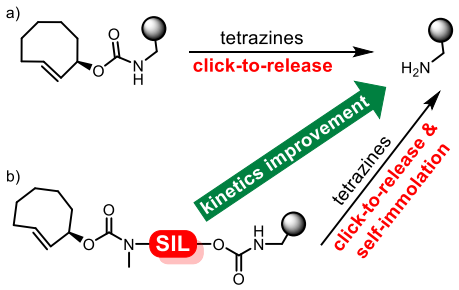

Figure 1. Comparison of the established click-to-release strategy (a) and the extended strategy for click-to-release experiments using self-immolative linkers (b).

For the first time in literature, it was possible to achieve almost quantitative release of primary amines. In addition, it was possible to determine the pH dependency (pH 4-9) with regard to the reaction rate of released compounds and to determine their optimum. The pH dependency on the kinetics of click-to-release and self-immolation emphasized again the importance of environmental sensitivity of the whole disassembly cascade.

Acknowledgement

First, I would like to thank Professor Johannes Fröhlich to conduct my master thesis in his research group.

Special thanks to both of my supervisors for their great support: To Hannes Mikula, who gave me the unique chance to work on a topic whose content I was able to identify with excellently. Also to Philipp Skrinjar for his outstanding ideas towards synthesis as well as his exceptional motivation and personal commitment. Without their help and understanding, neither my personal nor practical development would have been possible.

Thanks to Christian Hametner for the conduction of numerous NMR experiments and his brilliant support.

Furthermore, I want to extend my warmest thanks to the entire research group not only for the excellent atmosphere but also for their kind assistance.

Finally, my thanks also applies to my family, who never let me down and made what I am today.

Abbreviations

Besides common abbreviations of the English language as well as symbols of the chemical elements, all shortcuts listed below are used in this work. Onetime occurring acronyms are generally explained within the text.

b.r.s.m. ..... based on recovered starting material

$BF_3.Et_2O$ ..... boron trifluoride diethyl etherate

Boc ..... *tert*-butyloxycarbonyl

BODIPY-acid ..... 3-(4,4-difluoro-1,3,5,7-tetramethyl-4-bora-3a,4a-diaza-s-indacene-8-yl)-propionic acid

CA/P ..... citrate-phosphate

DIPEA ..... *N*,*N*-diisopropylethylamine

DMAP 4-dimethylaminopyridine

DMF ..... *N*,*N*-dimethylformamide

DMSO ..... dimethyl sulfoxide

DMT 3,6-dimethyl-1,2,4,5-tetrazine

EtOAc ..... ethyl acetate

GC/MS ..... gas chromatography / mass spectrometry (also termed GCMS)

HBTU ..... 2-(1*H*-benzotriazol-1-yl)-1,1,3,3-tetramethyluronium hexafluorophosphate

HPLC ..... high-performance liquid chromatography

HRMS ..... high-resolution mass spectrometry

IEDDA ..... inverse-electron-demand Diels-Alder

IPA ..... isopropanol

K7.HCl ..... 2-(6-(pyrimidin-2-yl)-1,2,4,5-tetrazin-3-yl)ethan-1-aminium chloride

LG ..... leaving group

Lys ..... lysine

MeCN ..... acetonitrile

MeOH ..... methanol

MPA ..... 3-(6-methyl-1,2,4,5-tetrazin-3-yl)propanoic acid

m-PEG7-amine 2,5,8,11,14,17,20-heptaoxadocosan-22-amine

NMR ..... nuclear magnetic resonance

NP ..... normal phase

PA_2 ..... 3,3'-(1,2,4,5-tetrazine-3,6-diyl)dipropionic acid

PBS ..... phosphate-buffered saline

PE ..... petroleum ether

pNP ..... *p*-nitrophenol

pNPCOCl ..... 4-nitrophenyl chloroformate

$PyrH_2$ ..... 2,2'-(1,2,4,5-tetrazine-3,6-diyl)bis(pyridin-3-ol)

RP ..... reversed phase

rt ..... room temperature

rTCO ..... releasing *trans*-cyclooctene

Ser ..... serine

SIL ..... self-immolative linker

SIL1 ..... *N*,*N*'-dimethylethane-1,2-diamine based SIL (also termed DMEDA-SIL)

SIL2 ..... 5-methyl salicyl alcohol based SIL (also termed phenolic-SIL)

TBAF ..... tetrabutylammonium fluoride

TBDMS ..... *tert*-butyldimethylsilyl

THF ..... tetrahydrofuran

TLC ..... thin layer chromatography

Tyr ..... tyrosine

UHPLC/MS ..... ultra high performance liquid chromatography / mass spectrometry (also termed LCMS)

General explanatory notes

Literature References

Literature quotes are cited as superscript Arabic numerals.

Substance Labeling

Compounds already described in literature are named according to their appearance in literature. Commercially available reagents used “as bought” were not numbered. Compounds unknown to literature that were prepared in the course of this thesis are numbered in bold Arabic numerals.

Nomenclature

The nomenclature of chemical compounds which are not described in the literature is based on abbreviations of connected or modified literature known compounds. Compounds known to literature, reagents or solvents might be described by simplified terms, common or trade names.

Table of contents

1 Schemes 1

1.1 Target compound for phenol release 2

1.2 Target compound for primary alcohol release 3

1.3 Target compound for primary amine release 4

2 Introduction 5

2.1 Bioorthogonal chemistry 6

2.2 Bioorthogonal release 6

2.3 Self-immolative linkers 10

2.3.1 Self-immolation based on elimination 11

2.3.2 Self-immolation based on cyclization 12

3 Results and Discussion 14

3.1 Scope of this thesis 15

3.2 Synthesis of target compounds 18

3.2.1 Target compound for phenol release 19

3.2.2 Target compound for primary alcohol release 21

3.2.3 Target compound for primary amine release 23

3.3 Kinetic investigations 27

3.3.1 Phenol release upon click-to-release & self-immolation 28

3.3.2 Primary alcohol release upon click-to-release & self-immolation 32

3.3.3 Primary amine release upon click-to-release & self-immolation 33

4 Conclusion and Outlook 37

4.1 Conclusion 38

4.2 Outlook 38

5 Experimental Section 40

5.1 Materials and Methods 41

5.1.1 Reactants and Solvents *41*
5.1.2 Chromatographic Methods *41*
5.1.3 NMR Spectroscopy *42*
5.1.4 High Resolution Mass Spectroscopy (HRMS) *42*
5.1.5 Release Experiments *43*
5.1.5.1 UHPLC/MS setup and instrument solvents 43
5.1.5.2 Analytical stock solutions and Buffers 43
5.1.5.3 LCMS sample preparation 44
5.1.5.4 Analytical LCMS analysis 44
5.2 Synthesis and Characterization of Substances 46
5.2.1 Target compound for phenol release *46*
5.2.1.1 Tyr(OMe)-BODIPY (1) 46
5.2.1.2 pNP-Tyr(OMe)-BODIPY (2) 47
5.2.1.3 rTCO-SIL1-Tyr(OMe)-BODIPY (3) 48
5.2.1.4 rTCO-SIL1-Tyr(mPEG7)-BODIPY (4) 50
5.2.2 Target compound for primary alcohol release *52*
5.2.2.1 Ser(OMe)-BODIPY (5) 52
5.2.2.2 Ser(mPEG7)-BODIPY (6) 53
5.2.2.3 rTCO-SIL1-Ser(mPEG7)-BODIPY (7) 54
5.2.3 Target compound for primary amine release *56*
5.2.3.1 pNP-SIL2-TBDMS (8) 56
5.2.3.2 rTCO-SIL1-SIL2-TBDMS (9) 58
5.2.3.3 rTCO-SIL1-SIL2-pNP (10) 60
5.2.3.4 BocLys(mPEG7)-BODIPY (11) 62
5.2.3.5 rTCO-SIL1-SIL2-Lys(mPEG7)-BODIPY (12) 63

1 Schemes

1.1 Target compound for phenol release

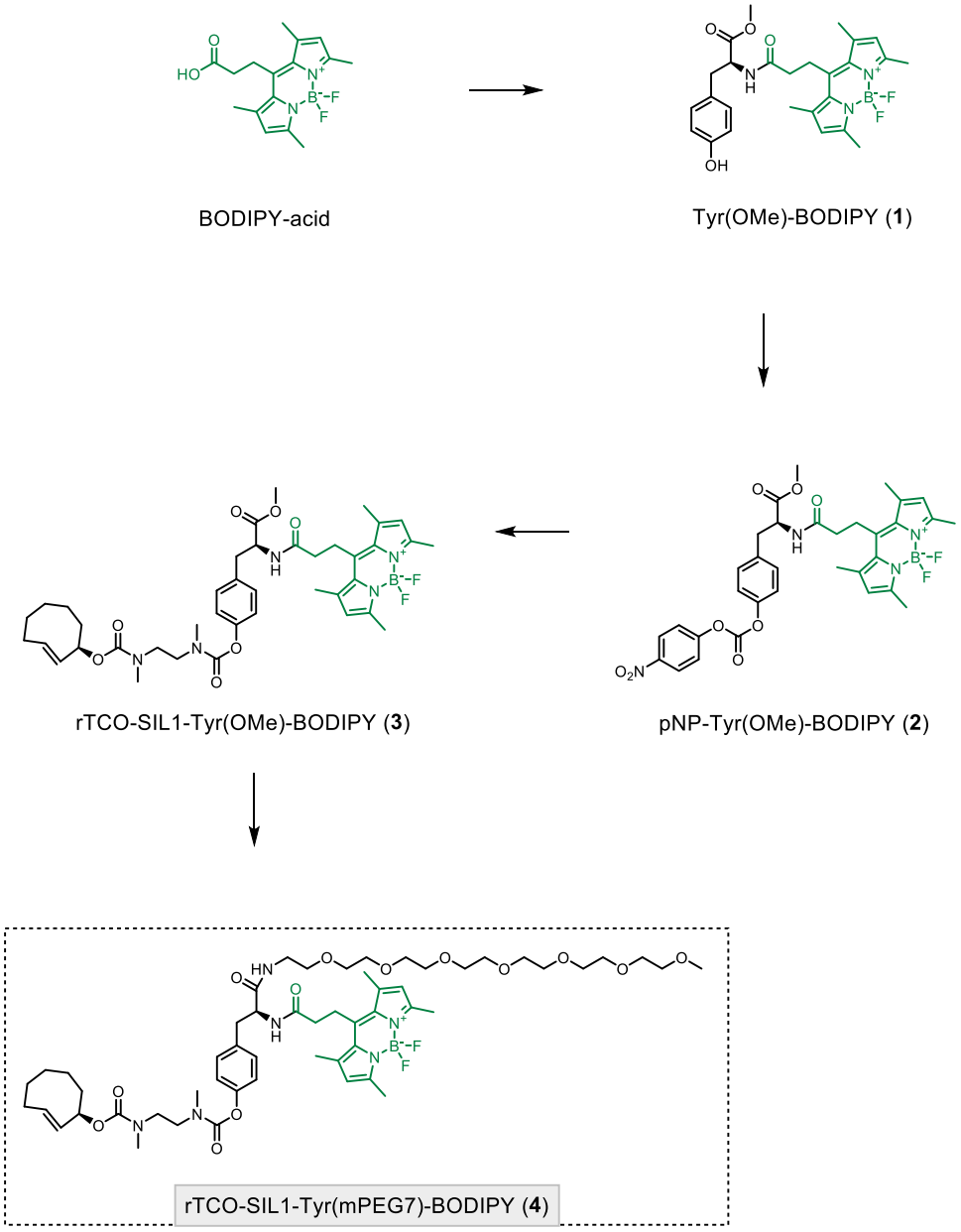

1.2 Target compound for primary alcohol release

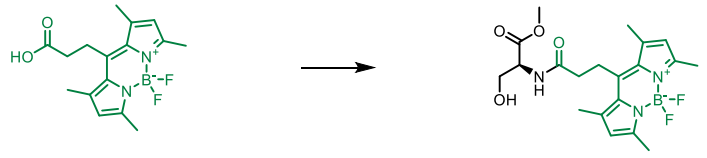

BODIPY-acid

Ser(OMe)-BODIPY (**5**)

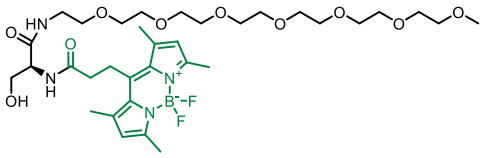

Ser(mPEG7)-BODIPY (**6**)

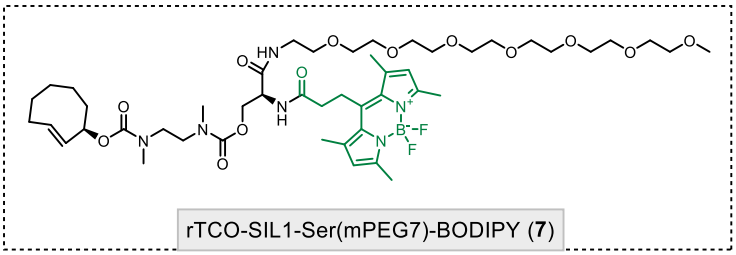

rTCO-SIL1-Ser(mPEG7)-BODIPY (**7**)

1.3 Target compound for primary amine release

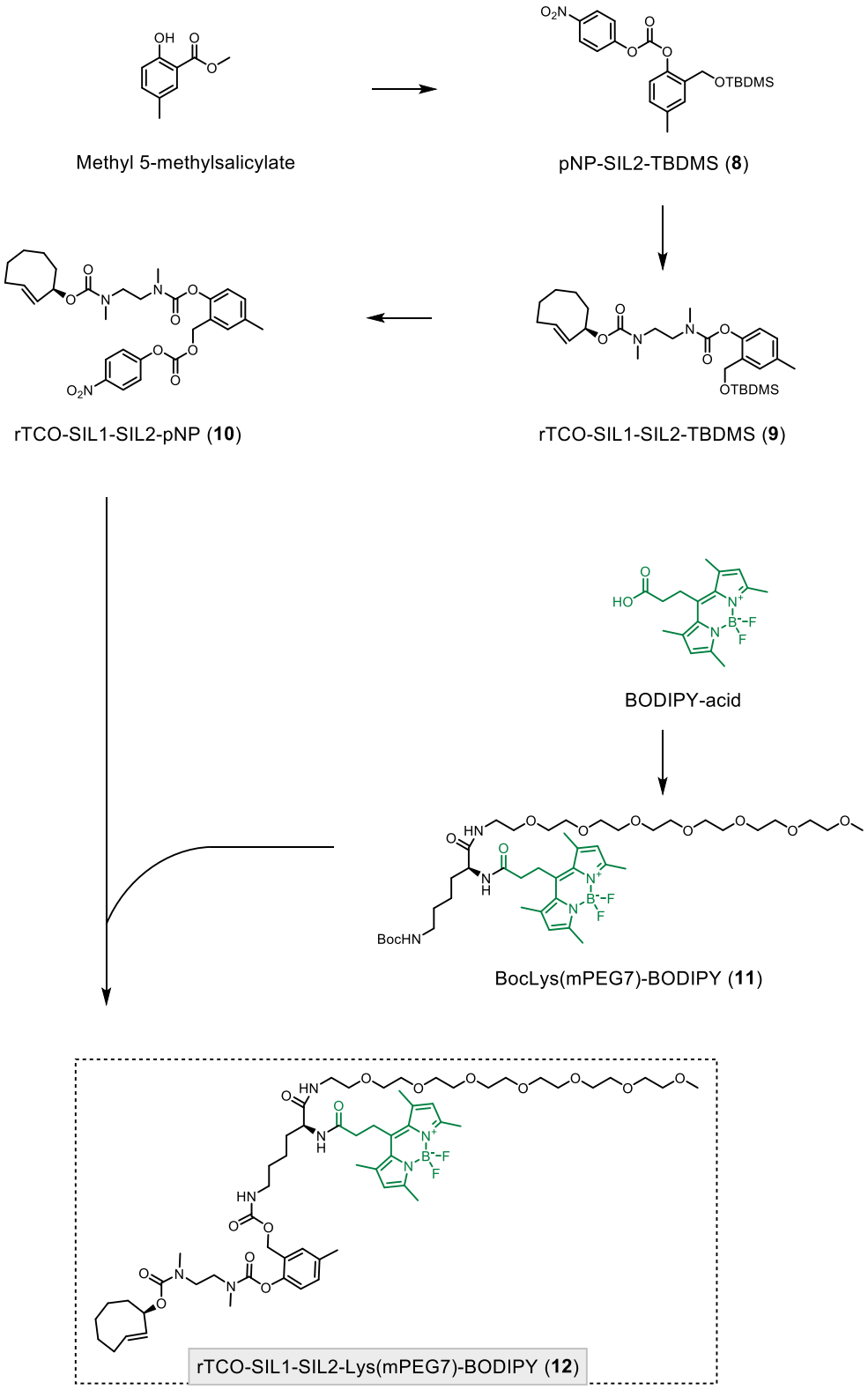

2 Introduction

2.1 Bioorthogonal chemistry

Firstly coined in 2003 by Carolyn R. Bertozzi[1], bioorthogonal chemistry refers to any reaction capable to neither interact nor interfere with biological systems. Feasible compounds must be inert to the variety of predominant functional groups found in biological systems, stable under physiological conditions and, especially in terms of *in vivo* applications, nontoxic to cells and organisms. Furthermore, selectivity and fast kinetics plays an indispensable role even though the concentration is addressed in the sub micro-molar range.[2–4]

2.2 Bioorthogonal release

Whereas bioorthogonal reactions since their introduction mainly focused on ligations like labeling,[5–8] tracking[9–12] and imaging,[13–21] the field of bioorthogonal reactions was expanded to enable cleavage of desired bonds. Cleavage reactions were sufficiently demonstrated on examples comprising the Staudinger ligation,[22] a palladium catalyzed[23] release or strain-promoted 1,3-dipolar cycloadditions.[24]

A new and breakthrough bioorthogonal “click-to-release” elimination reaction was developed by Marc S. Robillard[25] in 2013 that meet the criteria[26] of bioorthogonality with regard to rapid kinetics as well as biocompatibility. In their research they showed that the reaction between an allylic functionalized *trans*-cyclooctene (termed releasing TCO, rTCO) and tetrazine derivatives proceeds within an inverse-electron-demand Diels-Alder (IEDDA) reaction (Figure 2), leading to self-immolative release and renders release of desired carbamates possible. Activation after formation of initial 4,5-dihydropyridazine click adduct by reacting with tetrazine derivatives and subsequent loss of N_2 is continued by rapid tautomerization to 1,4- and 2,5-dihydropyridazines. The 1,4-tautomer is followed by an electron cascade elimination by shifting the N´s electron lone pair into the cyclic moiety and eliminates an amine containing moiety and CO_2 via carbamate disassembly. Finally,

the exocyclic double bond in conjugation to the pyridazine ring is subsequently rearranged to an aromatic system.

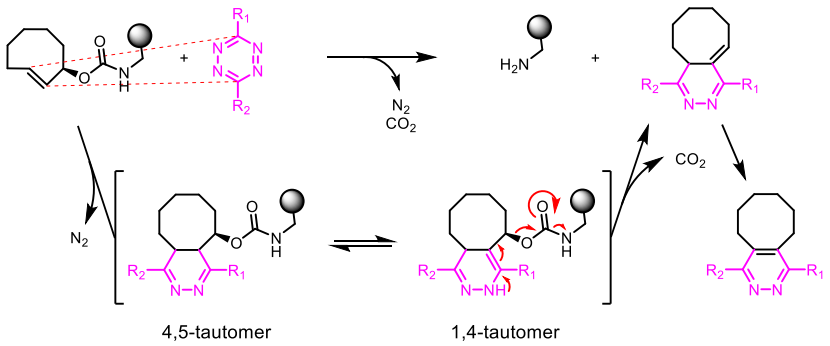

Figure 2. Simplified reaction between an allylic functionalized TCO (rTCO) and tetrazine derivatives leading to release of amines from the 1,4-tautomer by cleavage of carbamates: after activation within an inverse-electron-demand Diels-Alder cycloaddition the 4,5-dihydropyridazine is transferred via tautomerization to 1,4-dihydropyridazine releasing an amine upon an electron cascade elimination.

In their synthetic sequence based on (*Z*)-Cyclooct-2-en-1-ol, they obtained 2 enantiomers with the hydroxyl group either axially (ax-rTCO) or equatorially (eq-rTCO) positioned after photoisomerization. It turned out that the reactivity is favored for the axially substitute by two orders of magnitude. Despite fast release and promising biocompatibility their system suffered from incomplete release but was successfully introduced in the recent years for in vivo activation of antibody-drug-conjugates,[27] prodrugs,[28] proteins[29] as well as other applications.[30,31]

Recently, Weissleder[32] reported a detailed mechanistic investigation of the click-to-release mechanism in which the formation of a tricyclic dead-end isomer was revealed as the reason for poor release. Illustrated in a postclick reaction network showing interconversion species and release (Figure 3), the formation of the dead-end isomer was revealed as the product of intramolecular cyclization. The initially formed click adduct thereby renders further release impossible. N-Me substitution of the carbamates lone pair to obtain full substitution prevents the formation of the dead-end isomer and enables complete release which affords secondary amines as cleavable groups. It would be of highly advantageous to fully cleave primary amines as well to gain quantitative transformations within biological systems. Furthermore,

it has been shown that release experiments need to be performed in buffered solutions, as release kinetics might differ due to environmental sensitivity of IEEDA reactions.

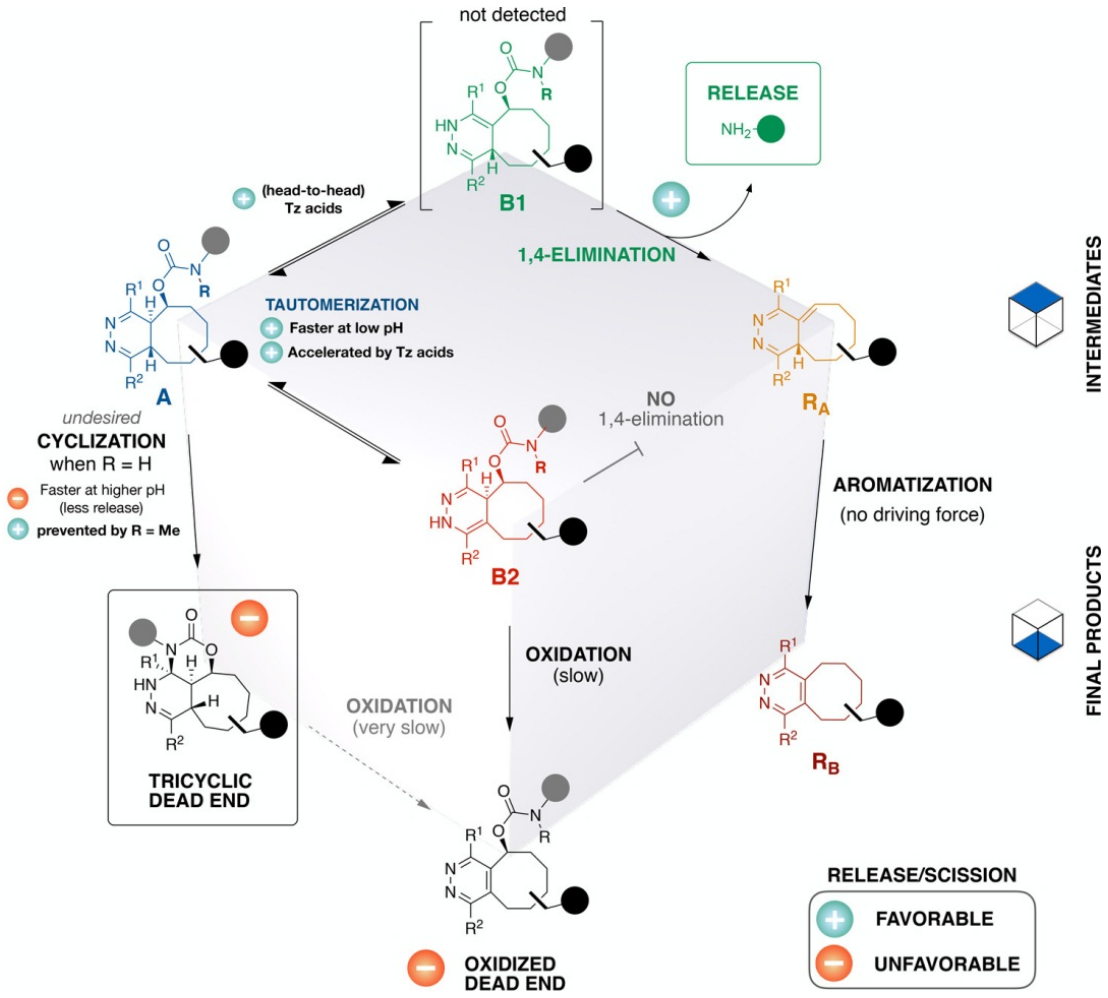

Figure 3. Mechanistic insights of the postclick network[32] showing interconversion species and release. The formation of a tricyclic dead-end species is the reason for poor release. Another dead-end caused by oxidation is only formed slowly. Remaining structures are identical to Figure 2.

The strong pH dependency of rTCO cleavage, which is favored in acidic environments, could be massively accelerated, in comparison to literatures standard tetrazine DMT, by acid functionalized tetrazines (MPA, PA_2).[32]

By introduction of aminoethyl functionalized tetrazines (K7.HCl, the fastest eliminating derivative, Figure 4) rTCO cleavage was made pH independent. Acting as

intramolecular catalyst for tautomerization, those tetrazines enhanced the elimination step throughout the pH range of physiological buffers.[33]

A remarkable and lately discovered pyridine-3-ol bis-substituted tetrazine derivative ($PyrH_2$) accelerated the click product formation to rTCO by a factor of 20 in comparison to DMT.

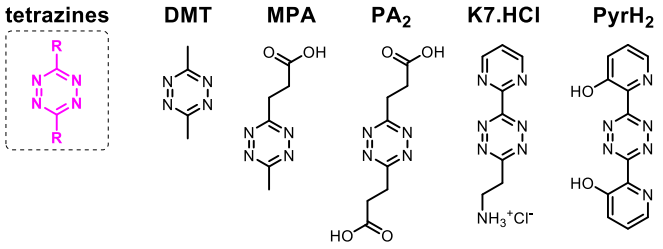

Figure 4. Established tetrazines for click-to-release experiments (selection): literatures standard tetrazine dimethyltetrazine (DMT), mono- (MPA)[32] and bispropanoic acid functionalized tetrazine derivatives (PA_2),[32] aminoethyl functionalized tetrazine derivative (K7.HCl)[33] and bis(pyridine-3-ol) tetrazine derivative $PyrH_2$.

Recently the scope of click-to-release reactions was expanded to cleave further functional groups besides carbamates. Again reported by Robillard[34], cleavage of esters, carbonates as well as primary alcohols and phenols linked to allylic functionalized *trans*-cyclooctenes model compounds was obtained. These findings provide a broad platform to envision novel innovative drug models that allow targeted release of payloads. But in respect of applying these techniques in living systems, bioorthogonality and stability of compounds is an essential factor. Especially sites of ligation like esters and carbonates are generally considered too labile for bioorthogonal applications.

As prodrugs are inactive or less active derivatives of the active drug they provide opportunities for directed cytotoxicity at target sites[35] albeit it is a challenge to selectively release them. rTCO linked diabody-based antibody-drug conjugates (ADC) were successfully targeted to tumor-associated glycoprotein-72 as cancer target in mice, followed by in vivo drug release upon tetrazine reaction. This strategy provided temporal and traceless drug release, minimized cytotoxicity[36] and

demonstrated the performance and challenges of recent developments in bioorthogonal chemistry.

2.3 Self-immolative linkers

Self-immolative linkers (SIL) are covalent moieties connected to a protecting group and a desired compound, designed to release the compound of interest after initial activation (Figure 5). Upon activation via cleavage of the protecting part of the non-releasing precursor, subsequent self-immolation within cascade reactions governs the release of the desired compound from SIL connectivity. Protecting group cleavage is based on chemical reagents, enzymatic activation or light irradiation.[37]

Since firstly reported in 1981 to overcome limitations in drug cleavage, using 4-aminobenzyl alcohol as a novel connector linkage,[38] self-immolation has found many usage regarding prodrug cleavage[39–44] and delivery.[43–46] Furthermore, it has been shown that if activation and release are suffering due to bulky sizes,[47] the application of SILs is a promising strategy against this limitation.[48]

Spatio-temporal control as well as additional payload increase by self-immolative dendritic amplifiers[49] in drug release experiments is of highly interest in this field of research. It is notably to consider that the application of self-immolative strategies

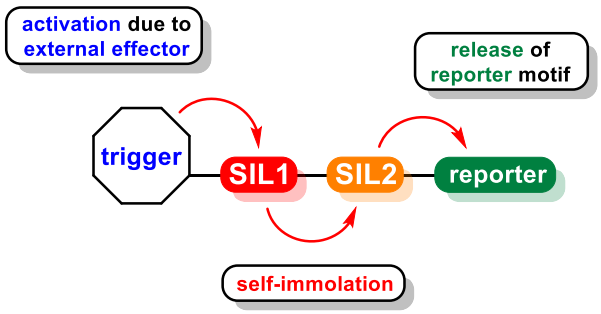

Figure 5. Connection setup of a SIL connected to its protecting group (trigger) and the compound of interest (reporter). Upon activation due to an external effector, the protecting moiety is removed leading to an activated species which decomposes spontaneous within several cascade reactions (self-immolation). At the end of the disassembly the active compound (reporter) is obtained. The scheme shows a linkage of two SILs.

could also directly change the properties of applied prodrugs, such as biological activity or water solubility.

Depending on the self-immolative structure used, self-immolation occurs either due to elimination- or cyclization-based mechanisms. Furthermore, combinations comprising both mechanisms in a sequence are also possible.

2.3.1 Self-immolation based on elimination

Self-immolation due to elimination (Figure 6) is based on an electron cascade in aromatic systems.[50–54] Deprotection of the capping moiety of weak nucleophilic compounds causes an enhancement in nucleophilicity, activating the precursor for its decomposition. Followed by a subsequent electronic cascade reaction via formation of intermediates, depending on the nature of the nucleophile, the desired compound is released. In addition to hydroxy or amino groups, also thiol groups can initiate the electron cascade after deprotection. The most common eliminations reported so far are 1,4-eliminations (Figure 6a) or 1,6-eliminations (Figure 6b). Electronic cascade eliminations towards extended aromatic systems are less successful due to greater energetic barriers.[55] Elimination reactions are driven by formation of thermodynamic stable products and positive entropy.

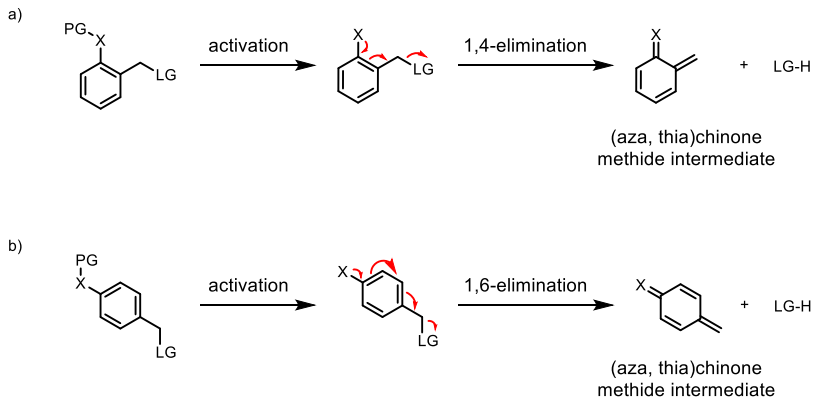

Figure 6. Schematic representation of a) 1,4-elimination[50–52] and b) 1,6-elimination-based[50,52–54] SILs (drawn without substituents). Upon cleavage of the protecting group reveals its intrinsic nucleophilicity that liberates the desired compound within an electronic cascade reaction in a) ortho- or b) para-delocalization. In case of hydroxy species, a quinone methide intermediate is formed, whereas an azaquinone methide respectively a thiaquinone methide intermediate is the result of amine or thiol species decomposition during the cascade elimination. PG = protecting group; X = O, NH or S; LG = leaving group.

Introduction of electron-rich substituents on aromatic systems accelerate self-immolation kinetics due to an increase in electron density capable of stabilizing dearomatization as well as positive intermediates formed within the cascade reaction.[56,57] Furthermore, the release of the leaving group proceeds even faster if the linkage is based on carbamates[51] instead of ethers and the benzylic position is substituted by methyl groups, again stabilizing the positive charge of the intermediate.[58] The leaving group quality improves with decreasing pK_a, affecting the speed of release.[59]

With increasing solvent polarity, the liberation of the leaving group is accelerated due to the stabilization of partial charges formed within the cascade reaction.[60] Another factor to be considered is the pH, which changes the ionization state and therefore the nucleophilic character of the deprotected nucleophiles.[51]

2.3.2 Self-immolation based on cyclization

Another mechanism that enables self-immolation is based on cyclization (Figure 7). Linkers which fulfill those criteria consist either of linear alkyl chains (Figure 7a)[61–64] or ortho-substituted aromatic systems (Figure 7b),[65–68] both equipped with carbonyl groups last attached. Upon deprotection, the activated linker undergoes a

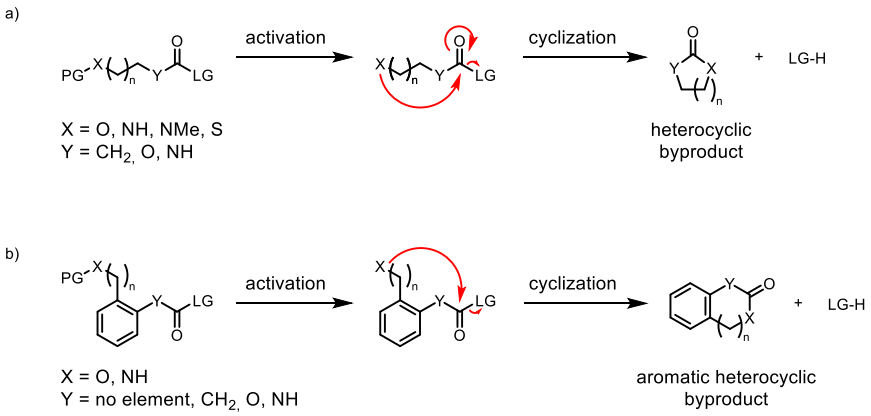

Figure 7. Schematic representation of cyclization-based SILs (drawn without substituents). Upon cleavage of the protecting group reveals its intrinsic nucleophilicity that liberates the desired compound within a S_N2t-mediated cyclization. In the case of linker based on a) alkyl chains,[61–64] heterocycles are obtained as byproducts whereas b) aromatic heterocycles result for ortho substituted aromatic systems.[65–68] PG = protecting group; LG = leaving group.

nucleophilic attack at the carbonyl group to release the desired compound within an S_N2t reaction, whereas heterocyclic derivatives or aromatic heterocyclic derivatives are obtained as by-products. SILs based on cyclization reactions are driven by formation of thermodynamic stable products (5- or 6-membered rings) and positive entropy.

Unlike elimination, the conformation of the spacer plays a major role. Hence a change in disassembly kinetics is derived from the extent to which conformation can be altered by introduction of substituents. Methylation at various sites[69] forces rapid spacer cyclization that can be attributed to the Thorpe-Ingold effect and/or the reactive rotamer effect.[70] Again, a decreasing pK_a of the leaving group strongly affects the release.[59] Another influence occurs for the pH, since release kinetics is based on pH-sensitive groups.

3 Results and Discussion

3.1 Scope of this thesis

It has been shown that there are numerous promising strategies for self-immolation in order to purposefully release a desired compound, with distinct options available to tune the kinetics, either by selecting a certain linker or modifying existing systems as well. First, the protective group, which captures nucleophilicity inherently, can be removed if necessary to initiate the self-immolation to release the desired compound. However, previous protecting groups based on chemical activation were suffering of being non-bioorthogonal. At the same time, the bioorthogonal release has recently provided excellent opportunities to gain quantitative release, possible by fine tuning. Thus, the introduction of the bioorthogonal rTCO moiety as a non-established protecting group towards self-immolative strategies is an encouraging approach to enhance release kinetics as well to provide complete release after activation by choosing an appropriate SIL (Figure 8).

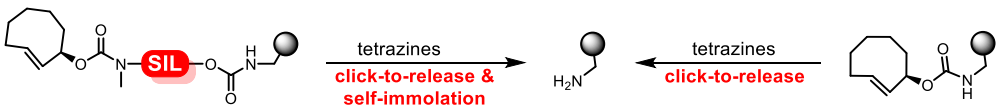

Figure 8. Comparison of the extended strategy for click-to-release experiments using self immolative linkers (left) with the classical click-to-release strategy (right) for the release of carbamates.

For bioorthogonal compatibility as well as for fast release, carbamates are still essential, as other functional groups suffer from either slow release or being non-entire bioorthogonal. To provide complete release by preventing the formation of a tricyclic dead-end isomer, N-Me substitution of the rTCO carbamates lone pair is indispensable. Therefore, self-immolative linkers equipped with a secondary amine are highly desirable, also in terms of synthesis. Depending on the nature of the desired leaving group, i.e. phenols, primary alcohols or primary amines, the carbamate linking the SIL and the desired leaving group, is also incorporated in reverse. In order to meet the requirements of aqueous kinetic investigations of molecule-disassembly, reporter motifs comprising enhanced hydrophilicity and a

fluorophore had to be extended at the target molecules. Since it has been questioned that the kinetics of self-disassembly in aqueous solution may differ from those of classical organic solvents,[32] a PEG chain was attached giving rise to obtain water solubility of target compounds at least at low concentrations. To enable quantification issues, the connection of a fluorescent dye is undeniable, allowing quantitative registration of all fragments during self-decomposition. Hence, a derivative of the well-established fluorescent dye BODIPY[71] (termed BODIPY-acid) was used (Figure 9).

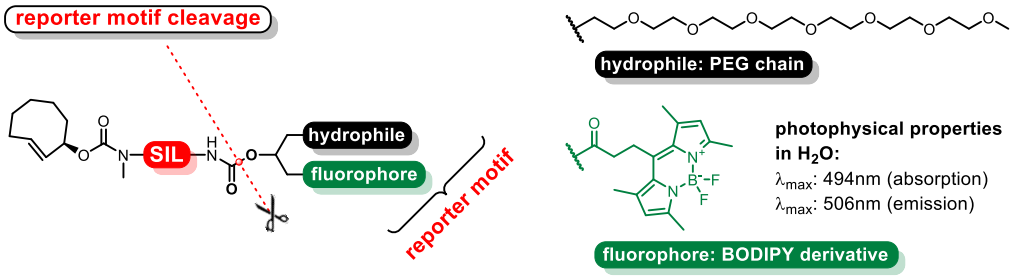

Figure 9. Structural connection setup to optimize limitations in terms of bioorthogonal compatibility, kinetics and complete release: Usage of carbamates to ensure bioorthogonal compatibility as well as fast release and N-Me substitution of rTCO´s carbamate to provide complete release. The introduction of a PEG chain ensures aqueous kinetic investigations, while the fluorescent dye of a BODIPY[71] derivative allows for quantification. Depending on the nature of the leaving group, the carbamate linking the SIL and the reporter motif is also incorporated in reverse.

By requesting to release phenols, primary alcohols as well as primary amines within all conditions mentioned, 3 target molecules for click-to-release and self-immolation experiments were aimed.

A phenol releasing minimalist prototype molecule (Figure 10) was obtained by connecting ax-rTCO and a tyrosine reporter motif onto a cyclization-based SIL (SIL1, a *N*,*N*'-dimethylethane-1,2-diamine based SIL, also termed DMEDA-SIL). Upon cleavage of rTCO, the activated SIL should spontaneously decompose to a cyclic urea derivative and release the desired phenolic reporter motif. Since the strength of nucleophilic attack is a result of the nucleophilicity of the deprotected compound, the rate of self-immolation under ring formation might strongly depend on the pH of aqueous solutions.

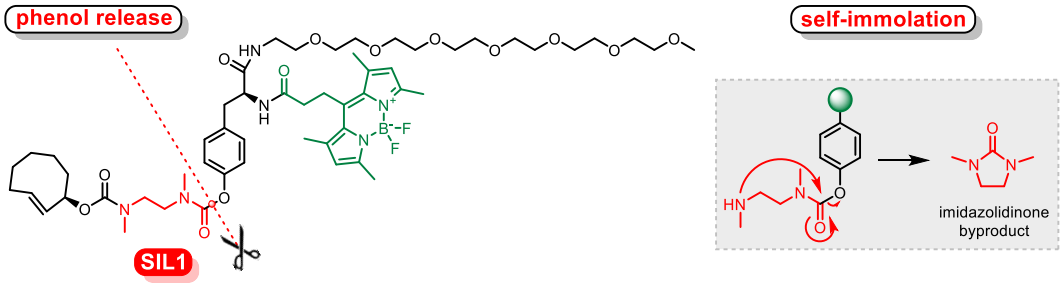

Figure 10. Target molecule for phenol release experiments: a cyclization-based SIL (red fragment, SIL1) connected to its rTCO protecting group and a phenolic reporter motif. Removal of the rTCO protecting group and subsequent spacer disassembly to a cyclic urea derivative should release the desired phenolic reporter motif as indicated.

The same connection setup applied for serine to obtain a target molecule for primary alcohol release experiments (Figure 11).

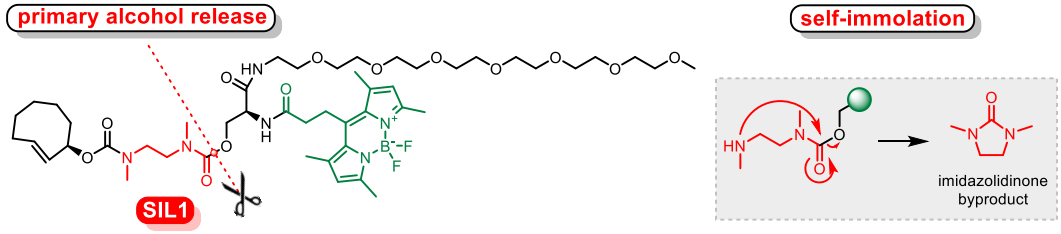

Figure 11. Target molecule for primary alcohol release experiments: a cyclization-based SIL (red fragment, SIL1) connected to its rTCO protecting group and a primary alcohol reporter motif. Removal of the rTCO protecting group and subsequent spacer disassembly to a cyclic urea derivative should release the desired primary alcohol reporter motif as indicated.

In terms of connectivity, it was more extensive to aim a prototype molecule for primary amine release (Figure 12) incorporating a linkage of two SILs. Again, by linking the cyclization-based SIL1 to ax-rTCO and in addition to an elimination-based SIL (SIL2, a 5-methyl salicyl alcohol based SIL, also termed phenolic-SIL) further connected to its corresponding reporter motif, a target molecule for primary amine release was accomplished. After initiating of the self-immolative cascade reaction, the activated SIL1 should spontaneously decompose to a cyclic urea byproduct releasing an activated SIL2 which upon elimination would give the desired reporter motif and a quinone methide intermediate. As already mentioned within the introduction of SIL1, a strong pH dependency of SIL1 and also SIL2 can be assumed.

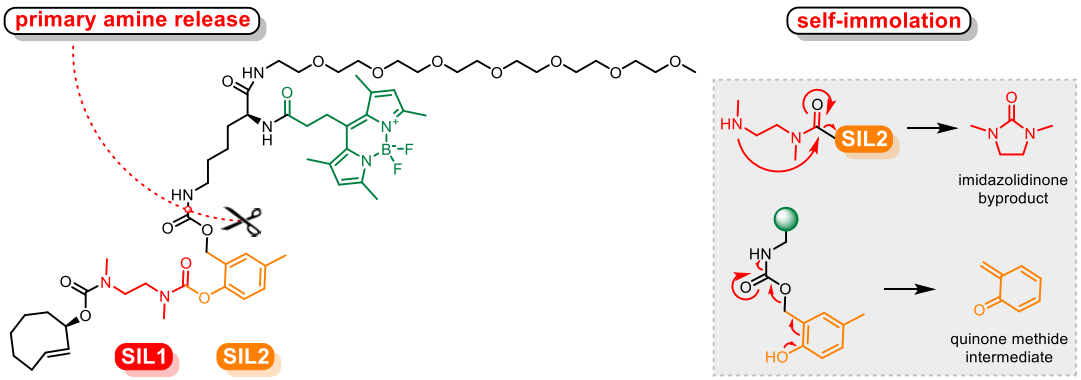

Figure 12. Target molecule for primary amine release experiments: a cyclization-based SIL (red fragment, SIL1) connected to its rTCO protecting group and to a further elimination-based SIL (orange fragment, SIL2) containing a primary amine reporter motif located at the end of the self-immolative cascade. Removal of the rTCO protecting group and subsequent spacer disassembly to a cyclic urea derivative as well as a quinone methide intermediate should release the desired primary amine reporter motif as indicated.

3.2 Synthesis of target compounds

With regard to the synthesis planning, introduction of SILs govern the order of synthetic steps applied, as unprotected motives bearing SILs naturally tend to decompose rapidly if handled inadequately. Additionally, the nature of protecting groups used must also be carefully considered to allow later deprotection in the presence of labile moieties like rTCO and BODIPY. The same applies to the amino acid containing fragment of the target compounds that is prone to epimerization at the α-position. However, especially the presence of the acid labile and easily re-isomerizing rTCO moiety made the synthesis challenging.

Furthermore, the necessity of protective groups occurred within the synthetic route, and protection was accomplished either by introduction of protecting groups or by using of commercially available compounds. Subsequent deprotection following conventional protocols often proved impossible. Therefore numerous attempts were required to identify suitable conditions, particularly with regard to the presence of sensitive moieties such as rTCO or BODIPY.

A simple and satisfying approach was found for the insertion of a cyclization-based SIL. It has been advantageous to establish the synthetic route following certain

pathways. Furthermore, it was shown that the synthesis or introduction of SILs is efficient with regard to one-pot strategies.

3.2.1 Target compound for phenol release

The synthesis begins with a HBTU mediated coupling of BODIPY-acid, a methylated BODIPY derivative comprising an acid functionality, to a methyl ester protected tyrosine to yield Tyr(OMe)-BODIPY **1** in excellent yield. Methyl ester protected tyrosine was used to avoid further coupling products of tyrosine.

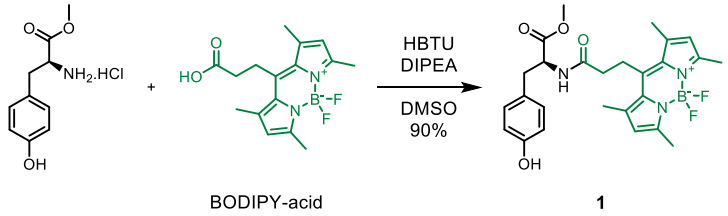

Figure 13. Synthesis of 1 by HBTU mediated coupling of methyl ester protected *L*-tyrosine and BODIPY-acid.

Subsequently, the synthesis was continued with the introduction of a pNP carbonate on the phenolic hydroxy group. The activated pNP carbonate approach was chosen as the synthetic route for the preparation of carbamates, since the pNP carbonate is easily introduced and the conversion to N-methyl substituted carbamates by secondary amines is straightforward. Later within this work, carbamates were also prepared in terms of one-pot syntheses from the corresponding educts. pNP-Tyr(OMe)-BODIPY **2** was obtained in excellent yield.

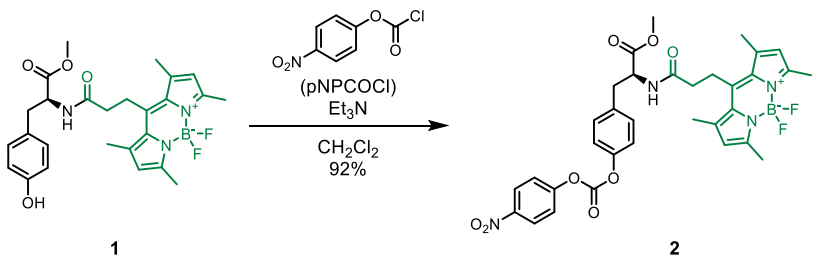

Figure 14. Synthesis of 2 by pNP carbonate activation of 1.

An excellent strategy emerged towards the insertion of the cyclization-based SIL1, which could be introduced within a one-pot synthesis containing previously connected rTCO and provided the required N-methyl group, necessary to prevent tricyclic dead-end formation. Initially, two pNP carbonates, consisting of rTCO and the desired leaving groups, were required to allow connection to the symmetric linker following a suitable order of events. To an excess of the diamino SIL1 precursor, rTCO-pNP was added first to acquire the monosubstituted amino compound rTCO-SIL1. After evaporation of the volatile diamino precursor, crude rTCO-SIL1 was obtained, which is stable at -20 °C for months. Addition of the pNP carbonate activated leaving group yielded the incorporated SIL1 as rTCO-SIL1-Tyr(OMe)-BODIPY **3** in good yield.

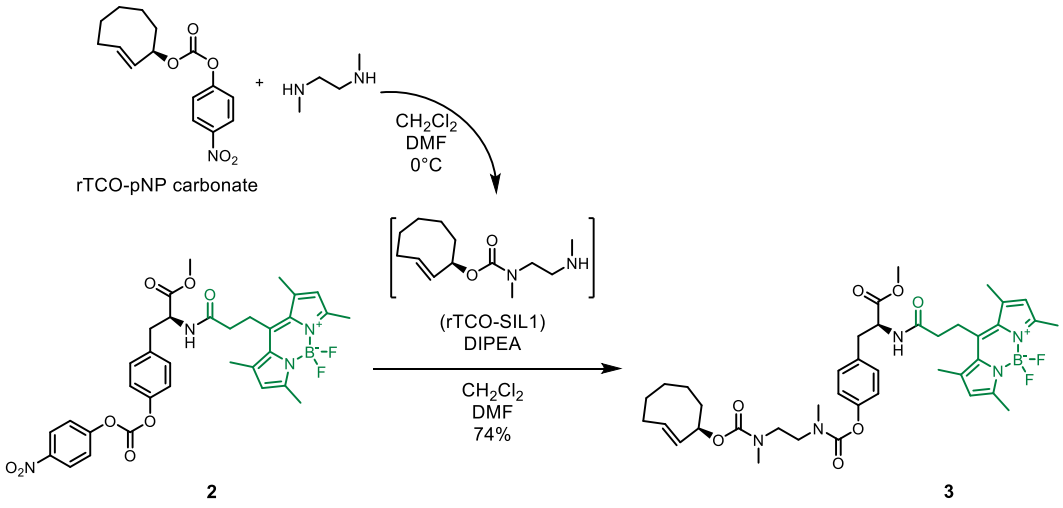

Figure 15. One-pot synthesis of 3 by introduction of the cyclization-based SIL1 onto 2.

The final step in the synthesis of the phenol releasing target compound involved the introduction of an amide linked PEG chain by replacing the methyl ester. The ester was deprotected following conventional saponification (KOH/water) to give free acid as an intermediate and finally the PEG chain was connected by HBTU mediated coupling. Due to solubility issues, the saponification was carried out in a solution containing water and IPA. rTCO-SIL1-Tyr(mPEG7)-BODIPY **4** was obtained in excellent yield.

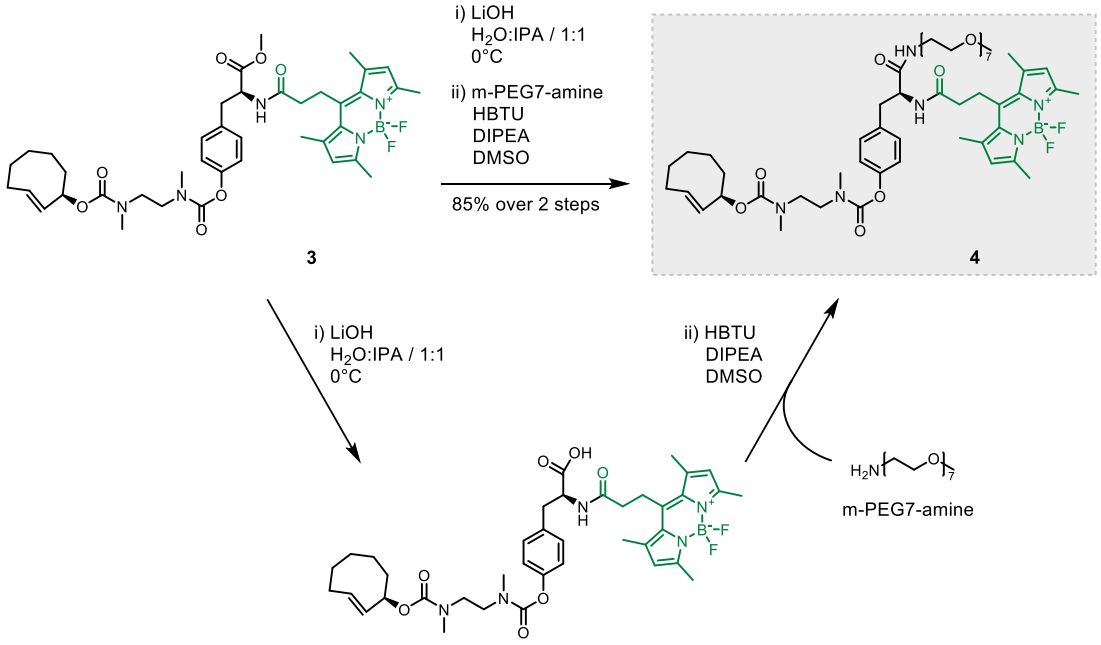

Figure 16. Synthesis of 4 by i) methyl ester deprotection of 3 and ii) HBTU mediated coupling of the free acid and m-PEG7-amine.

3.2.2 Target compound for primary alcohol release

HBTU mediated coupling of BODIPY-acid and methyl ester protected serine was prepared in an equivalent fashion to the procedure of the phenol releasing target compound to give Ser(OMe)-BODIPY **5** in excellent yield. Again, methyl ester protected serine was used to prevent formation of further coupling products.

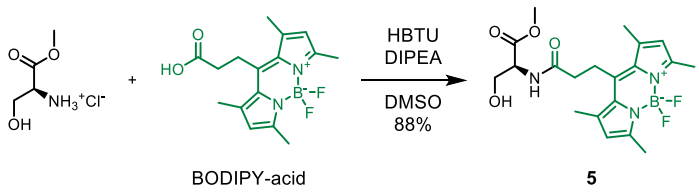

Figure 17. Synthesis of 5 by HBTU mediated coupling of methyl ester protected *L*-serine and BODIPY-acid.

Subsequent substitution of the methyl ester by an amide linked PEG chain proved to be challenging compared to the corresponding phenol approach due to formation of unknown intermediates upon deprotection. Thus, removal of the protecting group was performed very rapidly, as complete removal of the methyl

ester was achieved within a few minutes and resulted in the degradation of the free acid to various unidentified species over time. After HBTU mediated coupling to PEG, only a low yield of Ser(mPEG7)-BODIPY **6** was achieved.

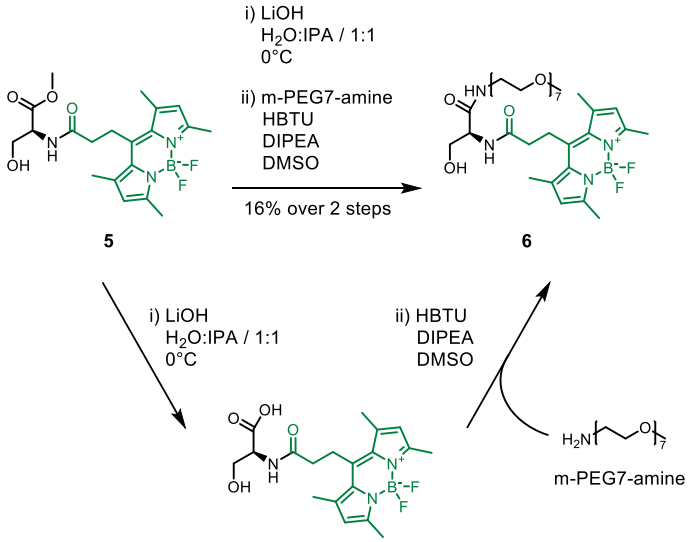

Figure 18. Synthesis of 6 by i) methyl ester deprotection of 5 and ii) HBTU mediated coupling of the free acid and m-PEG7-amine.

The insertion of SIL1 to synthesize rTCO-SIL1-Ser(mPEG7)-BODIPY **7** was obtained within a one-pot sequence. First, a pNP carbonate was introduced at the primary

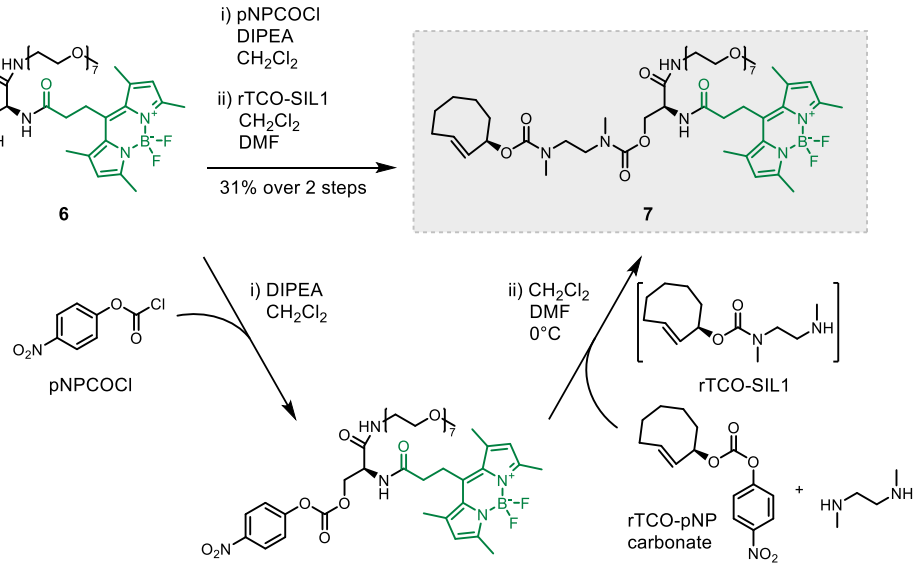

Figure 19. Synthesis of 7 by i) pNP carbonate activation of 6 and ii) insertion of the cyclization-based SIL1 within a one-pot sequence.

alcohol to allow subsequent carbamate formation by adding the SIL1 precursor. After incorporation of the rTCO-SIL1 precursor, the target compound for primary alcohol release experiments was obtained in moderate yield.

3.2.3 Target compound for primary amine release

For the design of a primary amine releasing compound that satisfies the need of preventing dead-end isomer formation only by releasing secondary amines while providing the opportunity to achieve complete release of primary amines, a SIL modification was inevitable. The established strategy for the insertion of SIL1 was applied, and an additional connection of a second SIL was required to invert the carbamate connection, allowing primary amine release.

The synthesis of a SIL2 precursor was based on a three stage synthesis. First, a salicylic acid derivative was reduced using $LiAlH_4$ to obtain a salicyl alcohol intermediate. Followed by regioselective TBDMS protection of the benzylic hydroxy group, the phenolic hydroxy group was activated by introduction of a pNP carbonate allowing the connection of amines. The precursor pNP-SIL2-TBDMS **8**

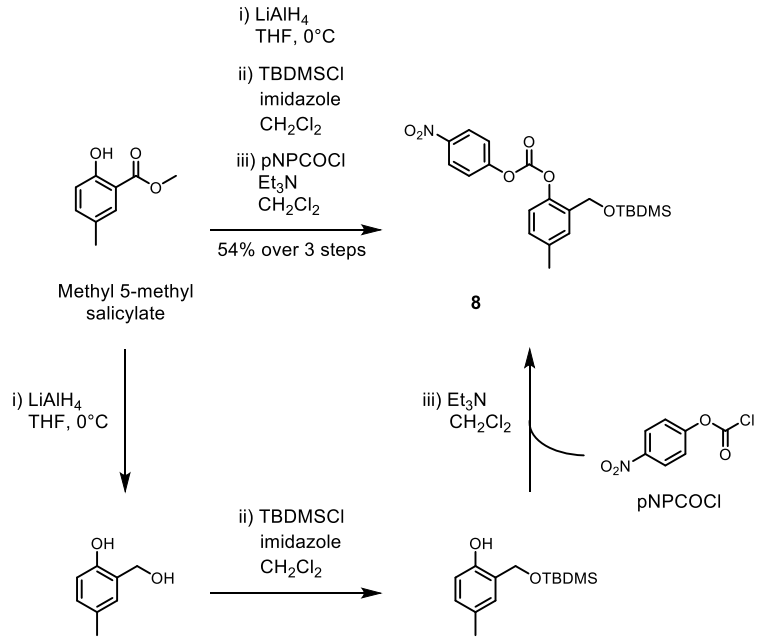

Figure 20. Synthesis of 8 by i) methyl ester reduction of a salicyl acid derivative, ii) TBDMS protection of the benzylic hydroxy group and iii) pNP carbonate activation of the phenolic hydroxy group.

was achieved in moderate yield.

Moving forward in synthesis, the SIL2 precursor and the crude rTCO-SIL1 intermediate, originating by selectively linking of rTCO to SIL1, were joined together. Again, the established strategy for the insertion of the cyclization based SIL1 within a one-pot synthesis gave an excellent yield of rTCO-SIL1-SIL2-TBDMS **9**.

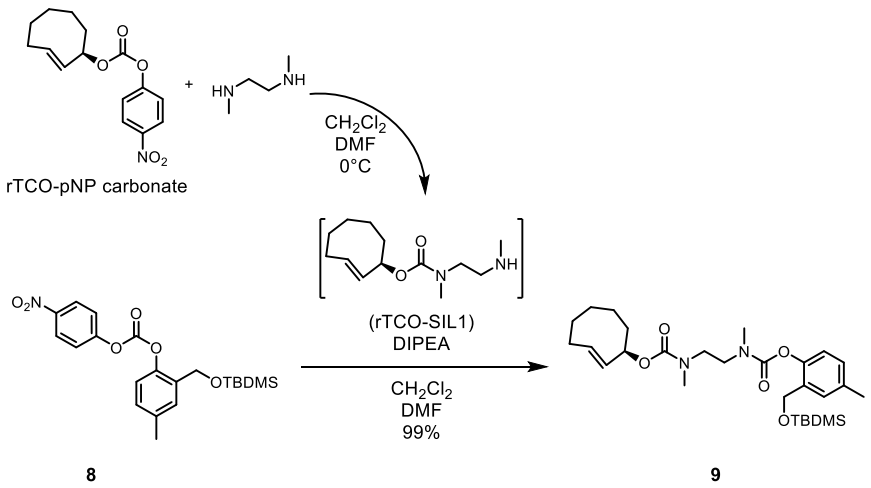

Figure 21. One-pot synthesis of 9 by introduction of the cyclization-based SIL1 onto 8.

TBAF mediated TBDMS deprotection of **9** initially proved difficult, as TBDMS deprotection following conventional methods (TBAF/THF) did not succeed. Only the preparation of a K_2HPO_4 buffered solution of TBAF in THF as well as lowering the reaction temperature to -5 °C successfully enabled TBDMS deprotection. Due to the rapid collapse of the compound at room temperature during deprotection, the reaction progress could not be easily monitored, causing the reaction to be quenched after 24 h. After a subsequent reaction to activate the benzylic hydroxy species via introduction of a pNP carbonate, unprotected TBDMS species **9** could be successfully separated and recovered after preparative HPLC. The synthesis of rTCO-SIL1-SIL2-pNP **10** proceeded with moderate yield and a quantitative b.r.s.m. yield upon recovering of **9**.

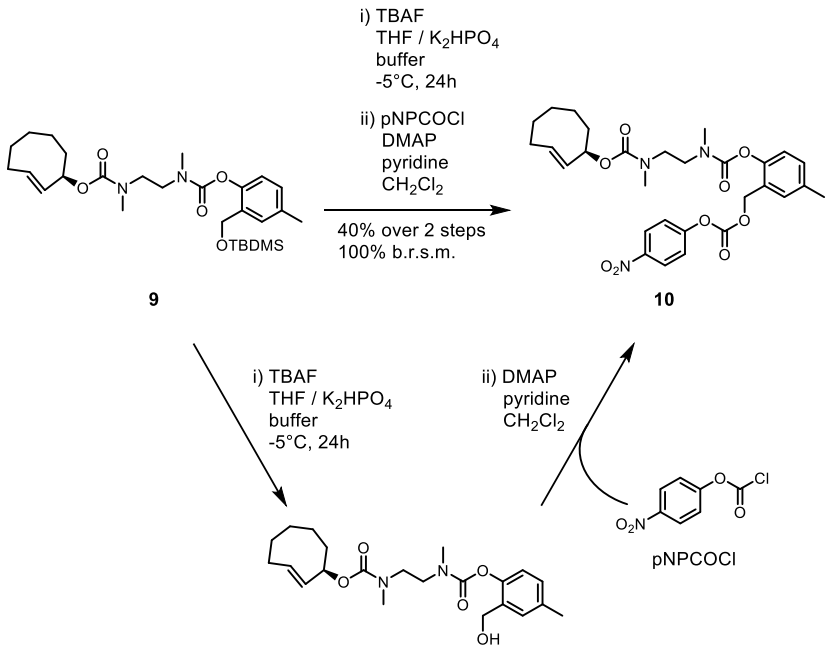

Figure 22. Synthesis of 10 by i) TBDMS deprotection of 9 and ii) pNP carbonate activation of the benzylic hydroxy group.

In order to obtain a reporter motif for the release of primary amines, BODIPY-acid was first reacted with N^{ε}-Boc protected *L*-lysine and subsequently with m-PEG7-amine in a one-pot synthesis of a HBTU mediated coupling reaction. Byproducts, of further coupled lysines, were separated by preparative HPLC and the Boc protected amine reporter motif, BocLys(mPEG7)-BODIPY **11** was obtained in moderate yield.

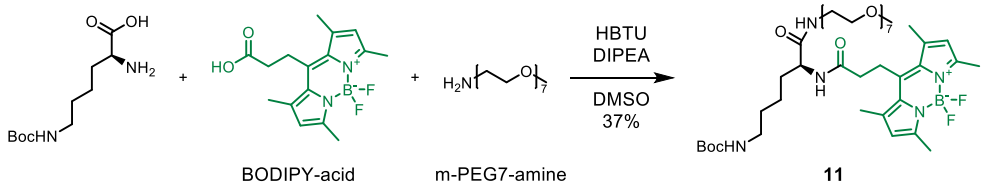

Figure 23. One-pot synthesis of 11 by HBTU mediated coupling of N^{ε}-Boc protected *L*-lysine, BODIPY-acid and m-PEG7-amine.

Lastly, the final step of the primary amine releasing target compound was based on a two stage synthesis. For this purpose, the Boc protected amine reporter motif was deprotected first using $BF_3.Et_2O$ to receive the free amine besides other species formed during deprotection. However, conventional TFA mediated Boc

deprotection did not lead to the desired product. The obtained primary amine reporter motif was then linked to the corresponding rTCO-SIL precursor **10** to give the target compound rTCO-SIL1-SIL2-Lys(mPEG7)-BODIPY **12** in low yield.

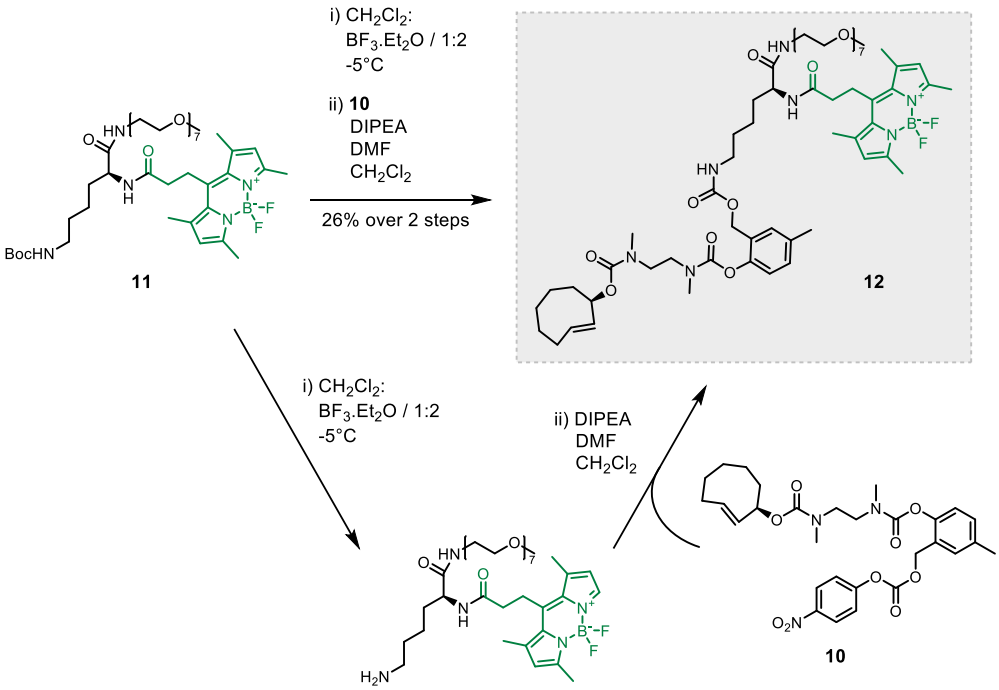

Figure 24. Synthesis of 12 by i) Boc deprotection of 11 and ii) insertion of the rTCO-SIL precursor for release of primary amines (10) onto the deprotected amine intermediate.

3.3 Kinetic investigations

The kinetic disassembly upon tetrazine mediated click-to-release of the target compounds was investigated with regard to the extent of physiological pH (citrate-phosphate (CA/P) buffer, phosphate buffered saline (PBS)).

Therefore BODIPY containing species of disassembly were identified by UHPLC/MS and their time dependent appearance or disappearance followed quantitatively via fluorimetry. Within all kinetic experiments performed, several BODIPY species appeared instantaneously after addition of tetrazines, which could not be assigned to expected disassembly cascade species (data not shown).

Two different SILs for the release of phenols respectively primary amines have been successfully introduced. Due to the fulfilled requirements regarding release efficiency, good or almost quantitative release was achieved within the duration of the 8 h experiments. Excellent kinetics was obtained for the release of phenols and primary amines. Release of primary amines was possible by a combination of two SILs. For the first time compared to literature data, almost quantitative release of primary amines was achieved.

In addition, it was possible to elucidate the pH dependency (pH 4-9) with regard to the reaction rate of released compounds and to determine the release optimum. The pH dependency on the kinetics of click-to-release and self-immolation emphasized again the importance of the environmental sensitivity. Since this was based on opposite pH dependent release kinetics, the reaction rate optimum of the reporter motif release was found to be a result of its individual processes.

Carbamate disassembly via carbamic acid decomposition as well as proton exchange was considered to be fast on the time scale of the kinetic experiments and thus rarely affected the overall process.

3.3.1 Phenol release upon click-to-release & self-immolation

Beginning with the first target compound, a phenolic reporter motif linked to rTCO via a cyclization-based SIL, a mechanism for the release cascade was proposed (Figure 25). Initially, by reacting one of the tetrazines used (DMT, MPA, PA_2, K7.HCl and $PyrH_2$), a click adduct is obtained immediately within the click-to-release strategy, capable of leading to different consecutive reactions depending on the

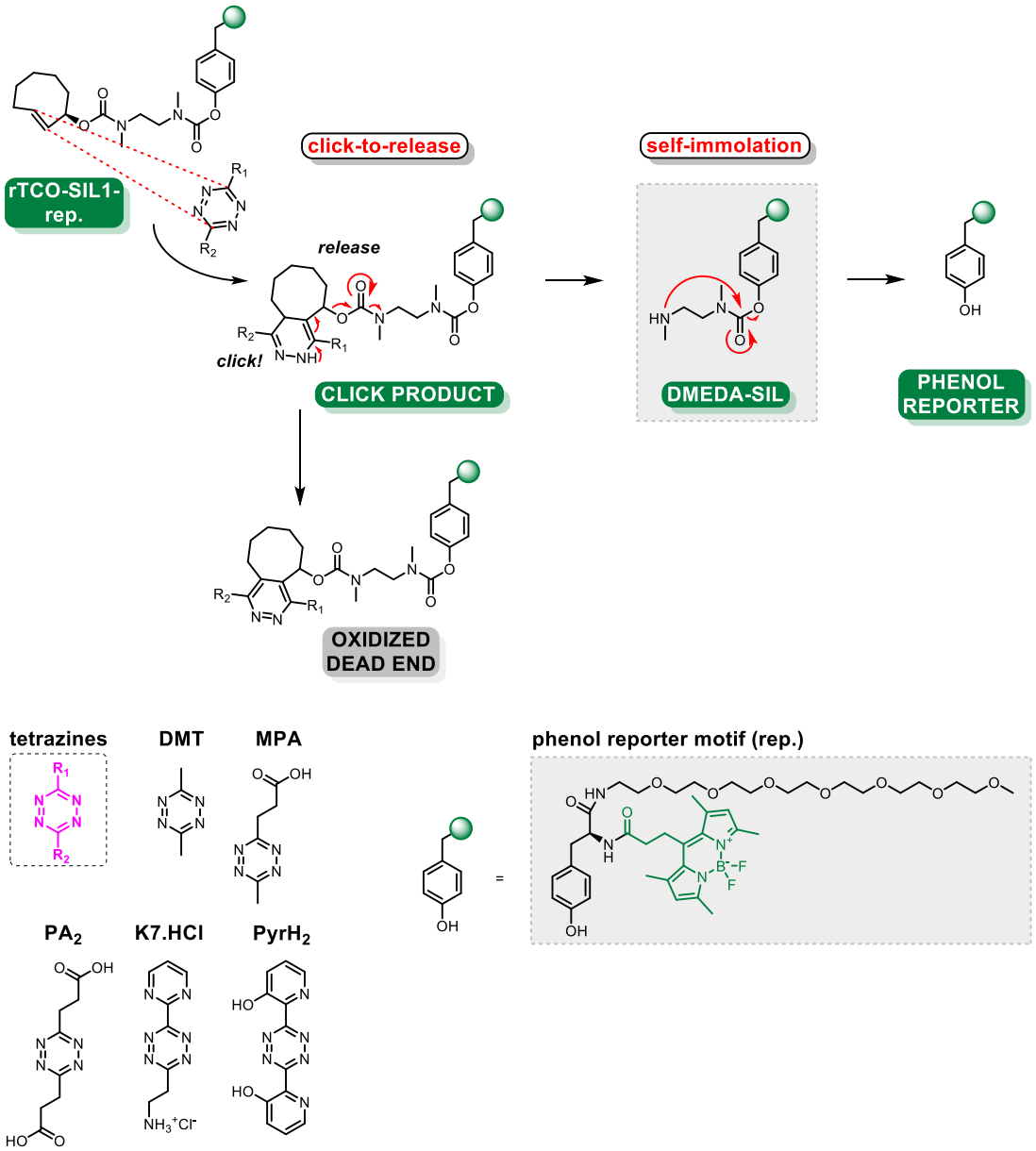

Figure 25. Proposed self-immolative mechanism for phenol release of a cyclization-based SIL: Upon reaction with tetrazine derivatives used, the initial click adduct leads to the release of an uncaged amine (DMEDA-SIL) via cleavage of carbamates. Subsequently the activated SIL is cleaved after self-immolation, resulting in the release of the final phenolic reporter motif. An oxidized dead-end species was not observed within all kinetic investigations performed. All intermediates contained BODIPY-labeled species.

tautomeric species (not shown). Via subsequent oxidation of the activated species leading to aromatization of the click adduct, would disable the self-immolative cascade. The oxidative dead-end is discriminated by a mass shift of 2 compared to the click adduct. Or, as the preferred second option available, in an electron cascade that eliminates rTCO and releases the activated linker, paving the way for self-immolation. Tricyclic dead-end formation is blocked by N-Me covered carbamates, which otherwise constitutes another side reaction as it was envisaged earlier (section 2.2). The activated cyclization-based linker (DMEDA-SIL) finally releases the phenolic reporter motif via S_N2t mediated cleavage within self-immolation.

Using DMT as the standard tetrazine for elucidating the pH dependence (pH 4-9) in CA/P buffer of the released species formed after click-to-release and self-immolation, a reverse course was observed (Figure 26). At pH 4, fast release of the DMEDA-SIL via rTCO cleavage was obtained, without any phenol release, even after hours. A shift to pH 5 enabled to release about 14 % in 7 h, with the free DMEDA-SIL dominating the species contribution. At pH 6, the release rate changed fundamentally, releasing about 65 % phenol within 7 h, with a small increase of rTCO cleavage time (1h). A significant enhancement in phenol release rate of the DMEDA-SIL was the result for pH 7, while the rTCO cleavage time was roughly doubled (2.5 h). The phenol release rate maximum was reached at pH 7.4 and a slightly reduced rate at pH 8. At the same time rTCO cleavage expanded even more (pH 8: 3.2 h) and the free DMEDA-SIL no longer dominated the species distribution. Further increase of pH led to prolonged rTCO cleavage times (pH 9: 4 h), with only low decrease in phenol release rate. For PBS at pH 7.4 a similar picture emerged than for CA/P buffer at pH 7, with higher release efficiency (90 % / 7 h).

Throughout the range of physiological pH, the DMEDA-SIL eliminated very sensitive with regard to pH, indicating the influence of protonation equilibria on the kinetics of self-immolation for cyclization-based SIL.

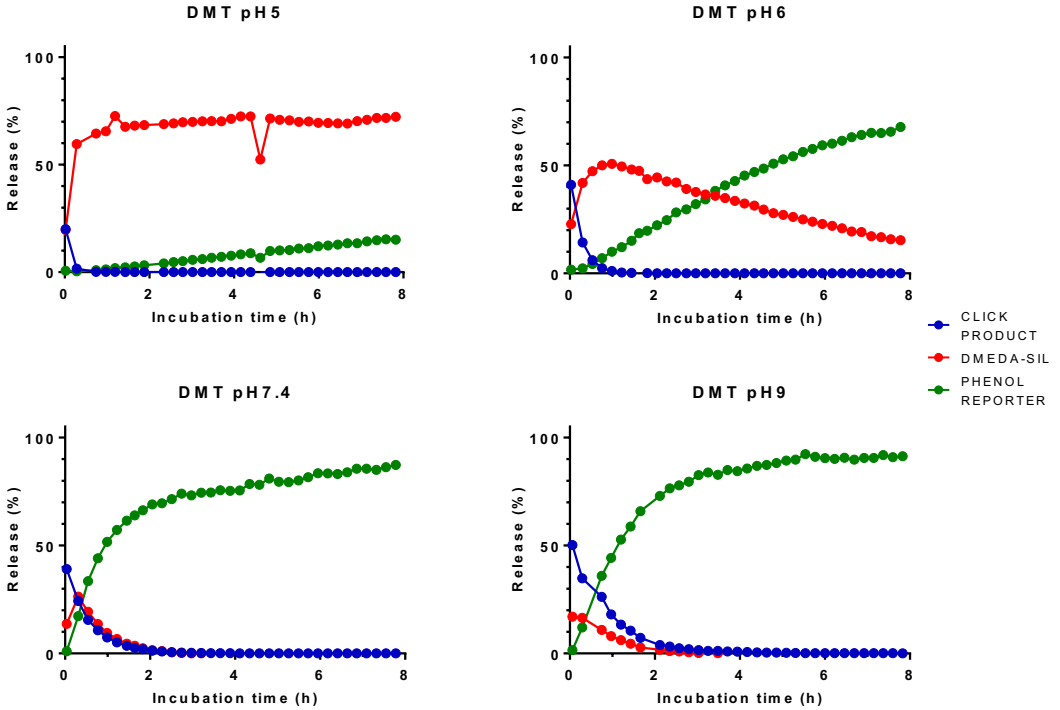

Figure 26. BODIPY labeled species distribution of phenol release in CA/P buffer (pH 5, pH 6, pH 7.4 and pH 9 at 37 °C) upon click-to-release and self-immolation mediated by DMT. Quantitative distributions of released fluorophore species were determined from fluorescent chromatograms, which were integrated at 500 nm and normalized to 100 %.

Furthermore, it was possible to determine the duration of pH dependent phenol release with respect to 80 % release (Figure 27). At pH 5, slow phenol release was observed, obtaining full release after >24 h. By contrast, pH 6 showed an

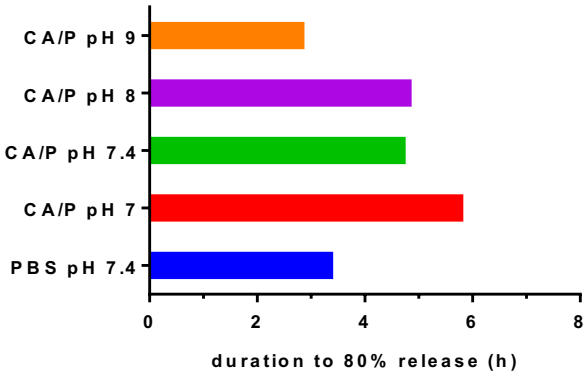

Figure 27. Duration of phenol release as a function of pH using DMT as initiator. Whereas only slow release was observed at pH 5 (>24 h, data not shown), a fundamentally release enhancement at pH 6 (<24 h, data not shown) was followed by an extensive acceleration of release kinetics within pH 7 to pH 9. A pronounced optimum at pH 9 was identified. PBS at pH 7.4 was similar to CA/P buffer at pH 9.

accelerated release within < 24 h. Among the rapid releasing pH window, emerging at pH 7-9, a phenol release optimum at pH 9 was identified. PBS at pH 7.4 obtained a similar release efficiency compared to CA/P buffer at pH 9.

By switching to faster releasing tetrazines MPA, PA_2, K7.HCl and $PyrH_2$, the release efficiency changed (Figure 28). Whereas the phenol release using acid-functionalized tetrazines MPA and PA_2 proceeded similar (MPA: 80 % / 6.6 h, PA_2: 80 % / 5.9 h), moderate release was found for K7.HCl (58% / 6.6 h), showing its usual performance. $PyrH_2$ exhibited initial fast release with an unexpected stop (58 % / 1.0 h, 70 % / 5.5 h).

The release of faster releasing tetrazines mainly accelerated the initial phase, followed by a slower releasing phase, which proceeded similar for all tetrazines. Compared to other tetrazines, PA_2 led to a slow asymptotic decline of DMEDA-SIL within pH 4-9.

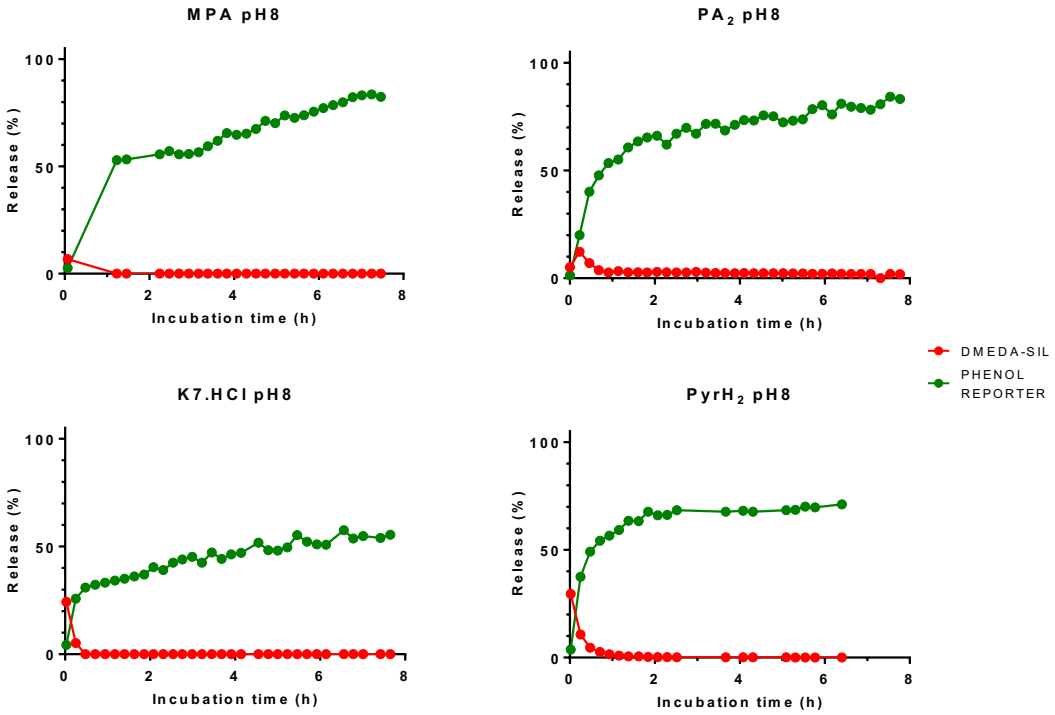

Figure 28. BODIPY labeled species distribution of phenol release in CA/P buffer pH 8 at 37 °C upon click-to-release and self-immolation mediated by MPA, PA_2, K7.HCl and $PyrH_2$. Quantitative distributions of released fluorophore species were determined from fluorescent chromatograms, which were integrated at 500 nm and normalized to 100 %.

3.3.2 Primary alcohol release upon click-to-release & self-immolation

An equivalent mechanism for click-to-release and self-immolation was proposed regarding the release of primary alcohols via a cyclization-based SIL (Figure 29). However, upon uncaging of the DMEDA-SIL, cleavage of the primary alcohol motif via a S_N2t mediated substitution could not be achieved, even at high pH, reflecting again its poor leaving group quality.

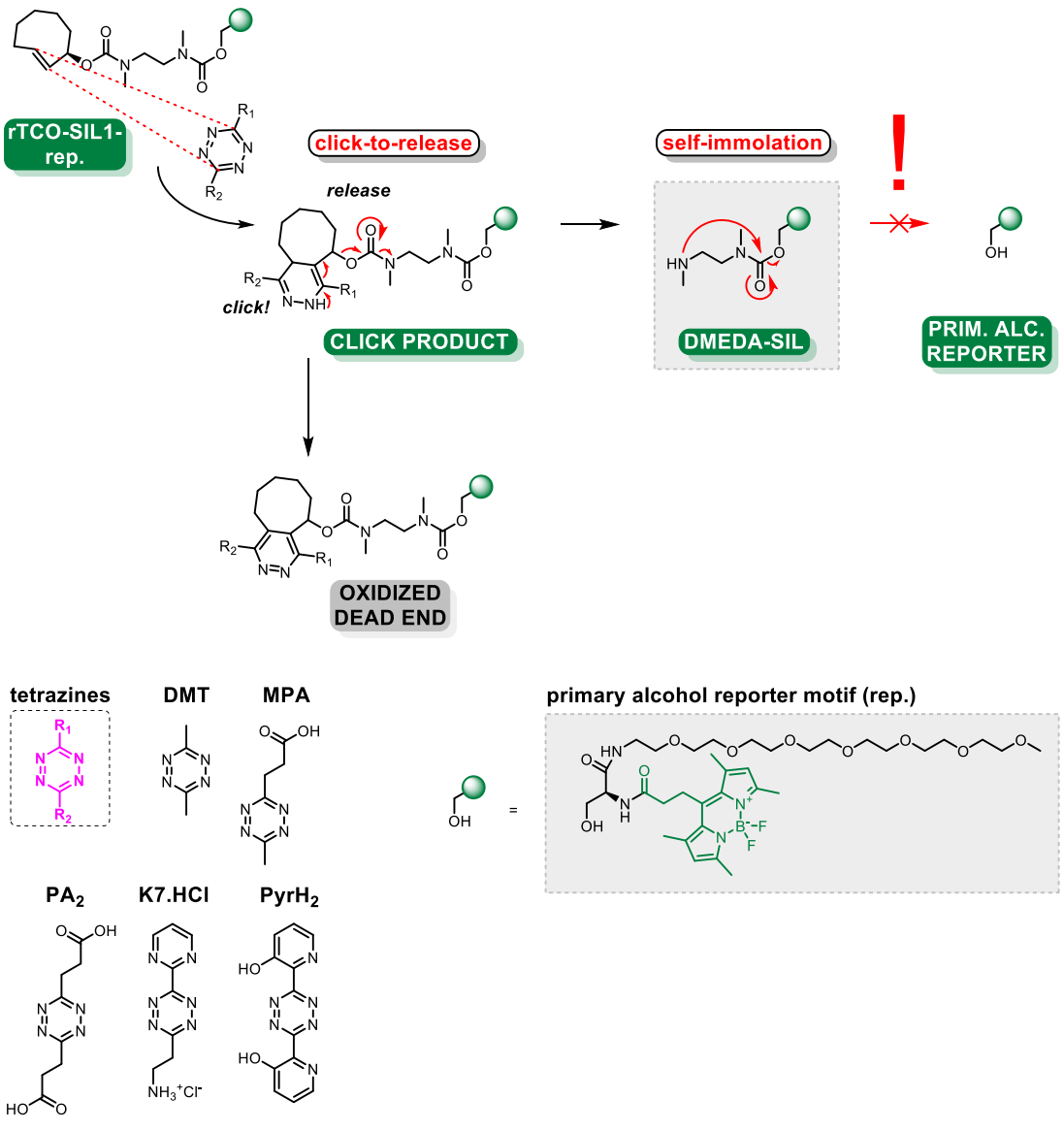

Figure 29. Proposed self-immolative mechanism for primary alcohol release of a cyclization-based SIL: Upon reaction with tetrazine derivatives used, the initial click adduct leads to the release of an uncaged amine (DMEDA-SIL) via cleavage of carbamates. Subsequently the activated SIL should be cleaved after self-immolation, resulting in the release of the final primary alcohol reporter motif. However, this was not the case. An oxidized dead-end species was not observed within all kinetic investigations performed. All intermediates contained BODIPY-labeled species.

3.3.3 Primary amine release upon click-to-release & self-immolation

Finally, a disassembly mechanism regarding a combination of a cyclization- and an elimination-based SIL, allowing for primary amine release, was proposed (Figure 30). After click product formation with tetrazine derivatives following the click-to-

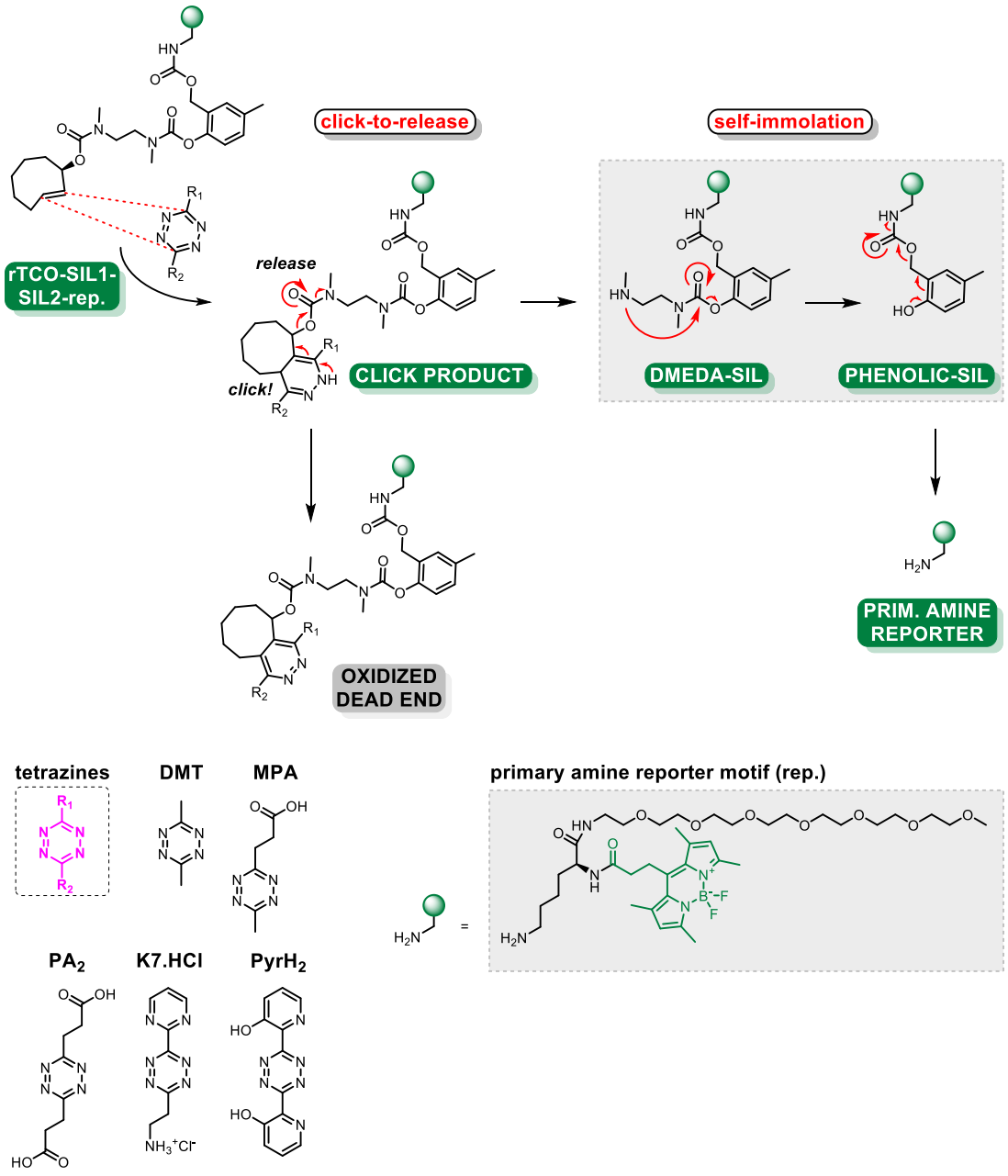

Figure 30. Proposed self-immolative mechanism for primary amine release of a combination of cyclization-based (SIL1) and elimination-based (SIL2) SILs: Upon reaction with tetrazine derivatives used, the initial click adduct leads to the release of an uncaged amine (DMEDA-SIL) via cleavage of carbamates. Subsequently the activated DMEDA-SIL is cleaved after self-immolation, resulting in the release of an activated phenolic-SIL that releases the final amine reporter motif after self-immolation. An oxidized dead-end species was not observed within all kinetic investigations performed. All intermediates contained BODIPY-labeled species.

release strategy, a cascade of spacer decompositions, as already explained (section 3.3.1), would either be disabled after click adduct oxidation or activated for subsequent SIL decomposition. Within the self-immolative cascade after cleavage of rTCO, the S_N2t mediated elimination (DMEDA-SIL) thereby rendering further release of an activated elimination-based SIL (phenolic-SIL). The 1,4-elimination-based SIL then eliminates the desired primary amine reporter motif last.

Looking at the kinetics of DMT mediated primary amine release upon click-to-release and self-immolation, equivalent pH dependence (pH 4-9) was found (Figure 31). However, primary amine release did not arise until pH 6. At pH<6, the reaction remained at the level of uncleaved DMEDA-SIL, and did not eliminate, even after hours. Again, rapid rTCO cleavage (0.5 h) was evident and a release of 26 % amine was achieved after 7 h at pH 6, with the DMEDA-SIL dominating the species contribution. A sharp improvement of primary amine release due to accelerated

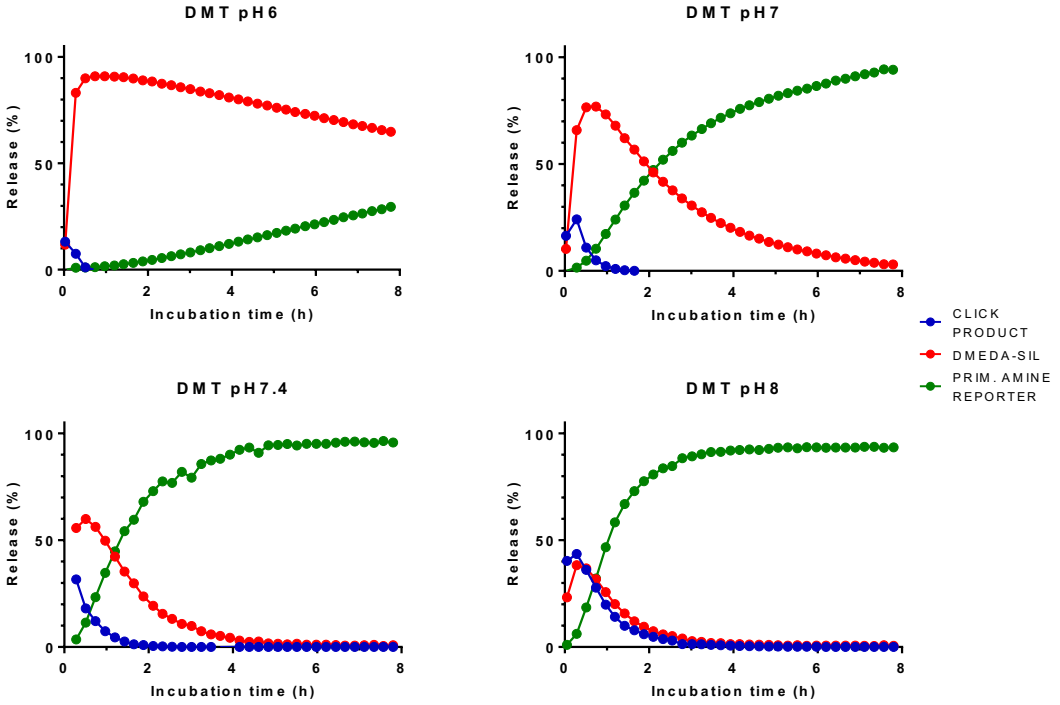

Figure 31. BODIPY labeled species distribution of primary amine release in CA/P buffer (pH 6, pH 7, pH 7.4 and pH 8 at 37 °C) upon click-to-release and self-immolation mediated by DMT. Quantitative distributions of released fluorophore species were determined from fluorescent chromatograms, which were integrated at 500 nm and normalized to 100 %. Within all kinetic measurements performed, no free phenolic-SIL was observed.

DMEDA-SIL cyclization occurred at pH 7, obtaining 92 % release after 7 h by simultaneous doubling of rTCO cleavage (1.5 h). Furthermore, the amine release efficiency increased at both pH 7.4 and pH 8 despite prolongation of rTCO cleavage (pH 7.4: 2.6 h, pH 8: 4.5 h) and was fastest at pH 8 offering 90 % release in 3 h. At the same time the DMEDA-SIL no longer dominated the species distribution. Within all kinetic measurements performed, no free phenolic-SIL was observed, emphasizing the rapid disassembly of the elimination-based phenolic-SIL in contrast to the cyclization-based DMEDA-SIL. The shift of pH dependency to higher pH must be related to an increased phenolic pK_a, compared to the phenol release in section 3.3.1, since an increased DMEDA-SIL nucleophilicity was afforded to cleave the leaving group. For PBS at pH 7.4 a similar picture emerged than for CA/P buffer at pH 7.

Moreover, it was possible to determine the duration of pH dependent primary amine release with respect to 90 % release (Figure 32). Despite nearly neutral conditions at pH 6, only slow release of primary amine was observed (~1 d). Contrary to that, neutral or slightly basic conditions provided continuous accelerated release efficiency. In conclusion, a primary amine release optimum was identified at pH 8.

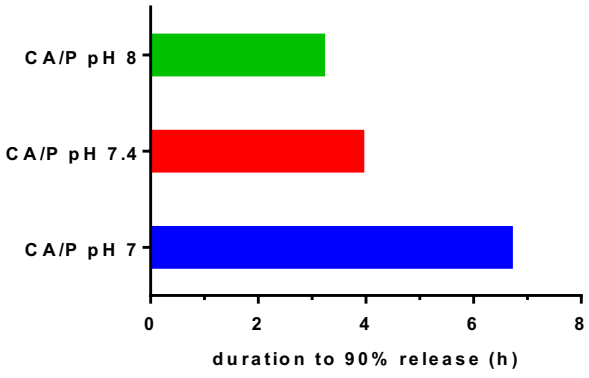

Figure 32. Duration of primary amine release as a function of pH using DMT as initiator. Whereas only slow release was observed at pH 6 (~1 d, data not shown), a fundamentally release enhancement at pH 7 was followed by further acceleration of release kinetics at pH 7.4 and pH 8. A pronounced optimum at pH 8 was identified.

Faster releasing tetrazines increased the rTCO cleavage efficiency at the release optimum (pH 8) demonstrating the rate limiting character of the self-immolative cascade (Figure 33). However MPA (88 % / 5 h) and PA_2 (83 % / 5 h) led to similar primary amine release efficiency (DMT: 93 % / 5 h). Moderate release was found for K7.HCl (81 % / 5.5 h), showing its usual performance. $PyrH_2$ exhibited initial very fast release and enabled almost quantitative release (65 % / 1.0 h, 95 % / 3.7 h).

Faster releasing tetrazines mainly accelerated the initial phase, followed by a slower releasing phase, which proceeded similar for all tetrazines. Again, compared to other tetrazines, MPA and PA_2 led to a slow asymptotic decline of DMEDA-SIL within pH 4-9.

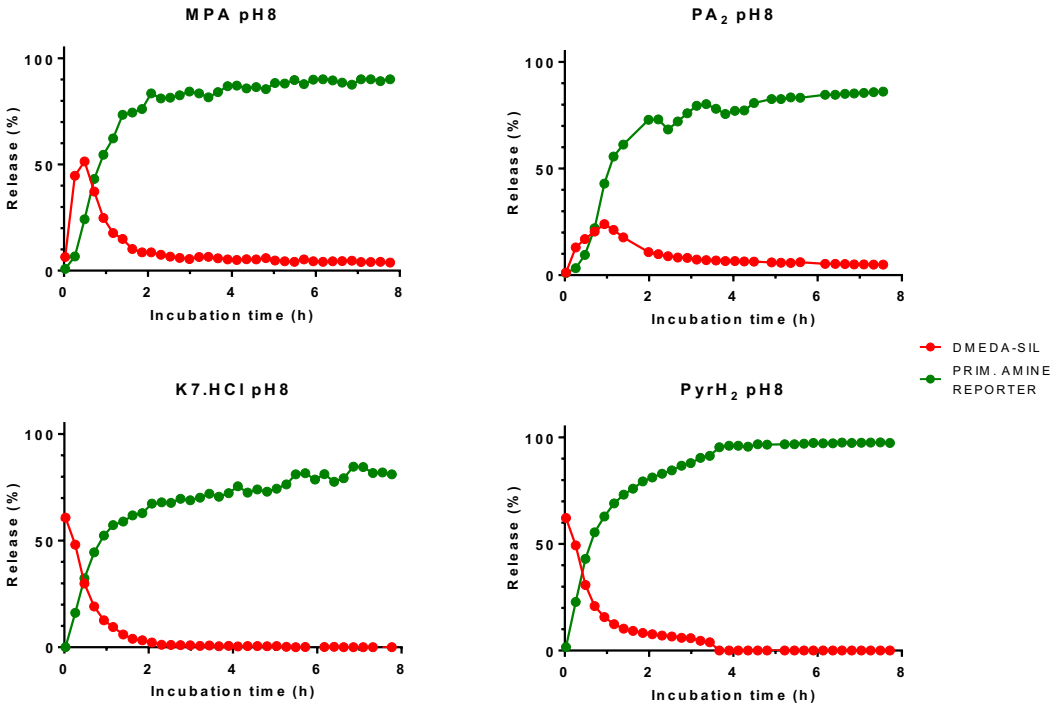

Figure 33. BODIPY labeled species distribution of primary amine release in CA/P buffer pH 8 at 37 °C upon click-to-release and self-immolation mediated by MPA, PA_2, K7.HCl and $PyrH_2$. Quantitative distributions of released fluorophore species were determined from fluorescent chromatograms, which were integrated at 500 nm and normalized to 100 %. Within all kinetic measurements performed, no free phenolic-SIL was observed.

4 Conclusion and Outlook

4.1 Conclusion

rTCO functionalized SILs for click-to-release of phenols respectively primary amines were sufficiently introduced. Evaluated systems achieved good or almost complete release of target compounds giving rise to potential future applications regarding bioorthogonal chemistry. In terms of performance, kinetics also showed an improvement in highly increased overall reaction rates. For the first time in literature, it was possible to achieve almost complete release of primary amines at highly accelerated kinetics. Furthermore, it was possible to elucidate the scope of physiological pH (pH 4-9) with regard to the reaction rate of released compounds and to determine their optimum. As expected viewed from different pH, acidic pH determined the elimination of the activated spacer as rate limiting step. Basic conditions favored self-immolation among simultaneous prolongation of rTCO cleavage, revealing its reaction rate maximum at slightly basic pH. Of particular importance was the combination of two SILs, which clearly identified the cyclization-based SIL as the rate limiting step.

4.2 Outlook

Due to the fact that primary alcohol release by self-immolation still remains unsolved, there is room for improvement here.

The overall release rate is governed by the speed of cyclization driven self-immolation. Thus, as reported[37], the introduction of hydroxy groups or cyclic moieties on the alkyl chain of the cyclization-based SIL allows to further accelerate the kinetics of self-immolation and therefore the overall cascade. In this context, also the use of methoxy-substituted arenes as ultrafast SIL, based on the concept of elimination is of highly interest.

For the release of primary amines, a simplified SIL comprising of a single SIL moiety is desired.

Expanding the field of bioorthogonal chemistry using self-immolative drug releasing strategies to cleave functional groups of interest is a prospect of the recent future.

5 Experimental Section

5.1 Materials and Methods

5.1.1 Reactants and Solvents

Unless otherwise noted, all reagents were purchased from commercial suppliers and used without further purification. CH_2Cl_2 and THF were dried using PURESOLV-columns (Innovative Technology Inc.). Dry acetonitrile (MeCN, Merck) and DMF (Acros) was commercially obtained and stored under argon. All other solvents were distilled prior to use. Drying of organic solvents after extraction was performed using anhydrous Na_2SO_4 (Sigma Aldrich) and subsequent filtration. Reactions were carried out under an atmosphere of argon in air-dried glassware with magnetic stirring. Sensitive liquids were transferred via syringe.

5.1.2 Chromatographic Methods

Thin layer chromatography was performed using TLC alumina plates (Merck, silica gel 60, fluorescence indicator F254). Visualization of the spots was achieved either by UV irradiation (254 or 366 nm) or by heat staining with ceric ammonium molybdate in ethanol/sulfuric acid.

Flash chromatography or preparative HPLC was carried out on a Grace REVELERIS® Prep purification system. The glass columns for flash chromatography were packed with silica gel 60 (Merck, 40-63 µm). For preparative RP-HPLC, (10 µm, C18, 100 Å, 250 x 21 mm) or straight phase-HPLC (10 µm, 100 Å, 250 x 21 mm) Phenomenex Luna columns were used. Mobile phases as well as quantities of silica gel respectively the type of column used (preparative HPLC), are mentioned in the corresponding synthesis.

GC/MS experiments were done with a Thermo Finnigan GC 8000 Top gaschromatograph on a BGB5 column (l=30 m, di=0,32 mm, 1 µm coating thickness) coupled to a Voyager Quadrupol mass spectrometer (electron ionization, 70 eV).

UHPLC/MS experiments for were performed on a Shimadzu® Nexera X2® comprising of LC-30AD pumps, a SIL-30AC autosampler, CTO-20AC column oven, DGU-20$A_{5/3}$ degasser module. Detection was accomplished by concerted efforts of SPD-M20A photo diode array, a RF-20Axs fluorescence detector, an ELS-2041 evaporative light scattering detector (JASCO®) and finally via a LCMS-2020 mass spectrometer. If not stated otherwise, all separations were performed using a Waters® XSelect™ CSH™ C18 2,5 µm (3.0 x 50 mm) Column XP at 40 °C, and a flowrate of 1,7 mL/min. Mobile phases used are HPLC-grade H_2O (0.1 % formic acid) and HPLC-grade MeCN (without additives), mobile phases used for release experiments see 5.1.5.1.

5.1.3 NMR Spectroscopy

^{1}H, ^{13}C NMR spectra were recorded on a Bruker Avance IIIHD 600 MHz spectrometer equipped with a Prodigy BBO cryo probe, on a Bruker Avance UltraShield 400 spectrometer or on a Bruker AC200 spectrometer at 20 °C. Chemical shifts are reported in ppm (δ) relative to tetramethylsilane and calibrated using solvent residual peaks. Data is shown as follows: Chemical shift, multiplicity (s = singlet, d = doublet, t = triplet, q = quartet, quin = quintet, sext = sextet, m = multiplet, br = broad signal) and integration.

5.1.4 High Resolution Mass Spectroscopy (HRMS)

HRMS analysis was carried out from aqueous THF solutions (concentration: 10 ppm) by using an HTC PAL system autosampler (CTC Analytics AG, Zwingen, Switzerland), an Agilent 1100/1200 HPLC with binary pumps, degasser and column thermostat (Agilent Technologies, Waldbronn, Germany) and Agilent 6230 AJS ESI–TOF mass spectrometer (Agilent Technologies, Palo Alto, United States). An Agilent 6230 LC TOFMS mass spectrometer equipped with an Agilent Dual AJS ESI-Source was used for the analysis. The mass spectrometer was connected to a liquid chromatography system of the 1100/1200 series from Agilent Technologies, Palo Alto, CA, USA. The system consisted of a 1200SL binary gradient pump, a degasser, column thermostat, and an HTC PAL autosampler (CTC Analytics AG, Zwingen, Switzerland). As

stationary phase a silica-based C18 column (4.6x50 mm) from Agilent and a Phenomenex C18 Security Guard Cartridge was used.

Data evaluation was performed using Agilent MassHunter Qualitative Analysis B.07.00. Identification was based on peaks obtained from extracted ion chromatograms (extraction width ± 20 ppm).

5.1.5 Release Experiments

5.1.5.1 UHPLC/MS setup and instrument solvents

For release experiments the autosampler temperature was set to 37 °C. The screening was carried out in injection intervals of 10 min, injecting 0.3-0.5 µL sample, depending on the saturation of the initial fluorescence signal.

For buffered LCMS conditions, the aqueous buffer was prepared by dilution of 625 µL of 10 M ammonium formate (BioUltra, Sigma-Aldrich) into 2.5 L of HPLC-grade H_2O and the pH adjusted to 8.5 with 100 µL of 25 % aq. ammonia (LiChropur®, Merck). HPLC-grade MeCN was used as the organic mobile phase. The pH of this volatile buffer declines over time and should be rechecked regularly, particularly if any drift in retention times is observed.

5.1.5.2 Analytical stock solutions and Buffers

Analytical stock solutions of the release probes **4**, **7** and **12** were prepared in H_2O under addition of 3 % DMSO, 3-fold higher than the final 50 µM target concentration for analytical LCMS assays, so that the final concentration of DMSO in buffer was exactly 1 %.

Tetrazine (DMT[25], MPA[32], PA_2[32], K7.HCl[33], $PyrH_2$) stock solutions were prepared in H_2O with a concentration 3-fold higher than the final 200 µM tetrazine concentration for analytical LCMS assays. In case of $PyrH_2$ 0.5 % DMSO were added to achieve complete dissolution.

CA/P buffers[72] were prepared by ratiometric dilution from standard stocks of 0.1 M citric acid and 0.2 M Na_2HPO_4 and their pH verified and adjusted as needed to within ±0.05 pH units by digital pH metering. 0.1 M buffers were diluted to give 30 mM buffers. 30 mM PBS was prepared directly from PBS tablets (Sigma-Aldrich).

5.1.5.3 LCMS sample preparation

Analytical samples for LCMS were prepared in a standard sequence: analytical stocks of release probes (30 µL) were diluted by micropipette directly into the relevant aqueous buffer (30 µL) in the LCMS sample vial micro insert and mixed, followed by addition of the tetrazine solutions (30 µL) to initiate the release cascade (time value set as t=0 h for kinetic experiments). Endpoint measurements were made at t ≥ 24 h.

5.1.5.4 Analytical LCMS analysis

Fluorescent data were collected for all samples and used to discriminate all signals containing the fluorophore tag from release byproducts. Quantitative distributions of released fluorophore species were determined from fluorescent chromatograms, which were integrated at 500 nm and normalized to 100 %.

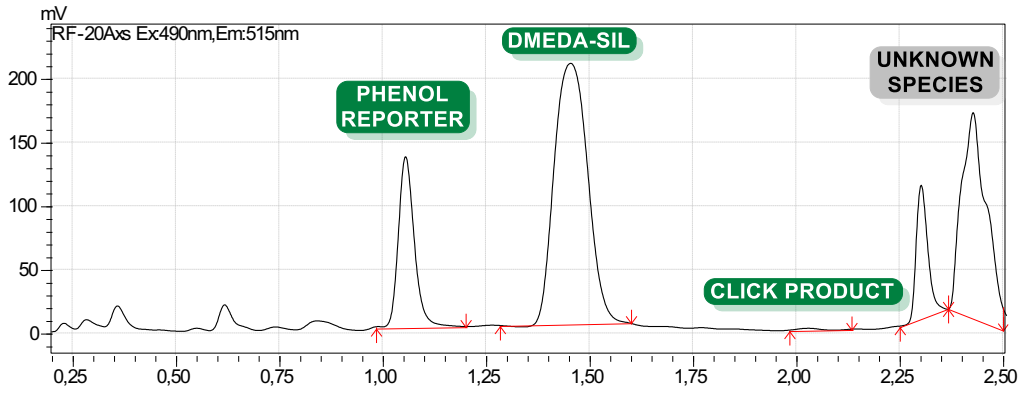

Figure 34. Fluorescent chromatogram of BODIPY labeled phenol release species in CA/P buffer pH 6 at 37 °C upon click-to-release and self-immolation (1 h 26 min 51 s after addition of DMT). Several BODIPY species could not be assigned to expected disassembly cascade species (t_R=2.25-2.50 min).

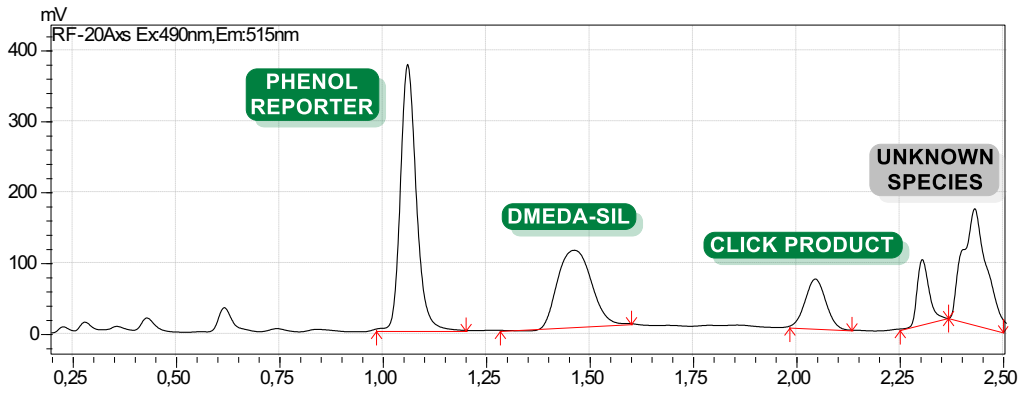

Figure 35. Fluorescent chromatogram of BODIPY labeled phenol release species in CA/P buffer pH 7 at 37 °C upon click-to-release and self-immolation (59 min 20 s after addition of DMT). Several BODIPY species could not be assigned to expected disassembly cascade species (t_R=2.25-2.50 min).

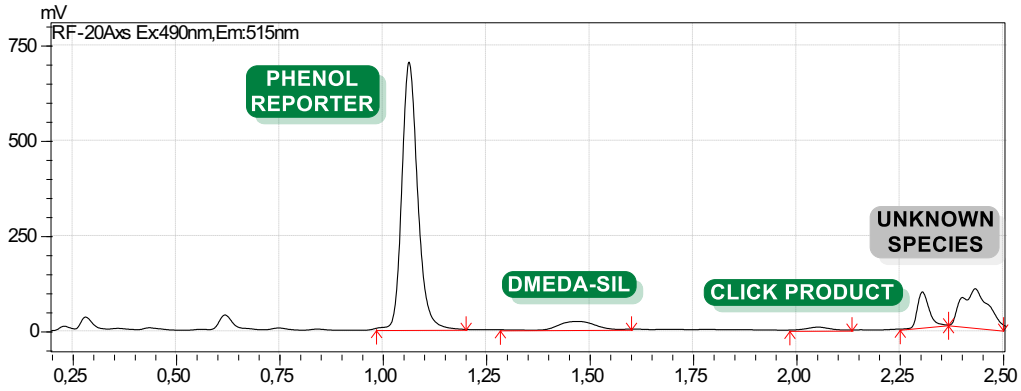

Figure 36. Fluorescent chromatogram of BODIPY labeled phenol release species in CA/P buffer pH 7 at 37 °C upon click-to-release and self-immolation (2 h 30 min 19 s after addition of DMT). Several BODIPY species could not be assigned to expected disassembly cascade species (t_R=2.25-2.50 min).

5.2 Synthesis and Characterization of Substances

5.2.1 Target compound for phenol release

5.2.1.1 Tyr(OMe)-BODIPY (1)

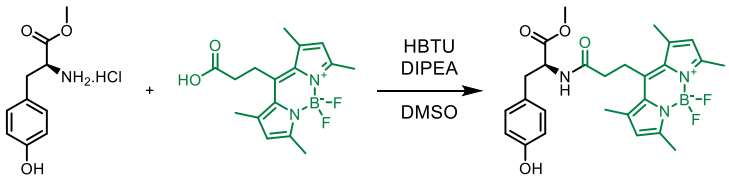

BODIPY-acid
$C_{16}H_{19}BF_2N_2O_2$
320.15

1
$C_{26}H_{30}BF_2N_3O_4$
497.35

To a solution of BODIPY-acid[71] (20 mg, 62.5 µmol) in DMSO (4 mL), *L*-tyrosine methyl ester hydrochloride (40.5 mg, 174.9 µmol), HBTU (35.5 mg, 93.7 µmol) and DIPEA (53.1 µL, 40.3 mg, 312 µmol) were added and stirred for 1 h at room temperature (rt). LCMS indicated complete conversion to the desired product. Purification by preparative RP-HPLC (H_2O/MeCN gradient elution, 0.1% formic acid) gave the desired product **1** as an orange solid (28.0 mg, 90%).

^{1}H NMR (600 MHz, CD_2Cl_2) δ 6.93 (d, *J* = 8.5 Hz, 2H), 6.73 (d, *J* = 8.5 Hz, 2H), 6.09 (s, 2H), 5.93 (d, *J* = 7.9 Hz, 1H), 5.23 (s, 1H), 4.81 (dt, *J* = 7.9, 5.9 Hz, 1H), 3.72 (s, 3H), 3.33 – 3.20 (m, 2H), 3.09 (dd, *J* = 14.0, 5.6 Hz, 1H), 2.97 (dd, *J* = 14.0, 6.1 Hz, 1H), 2.52 – 2.37 (m, 14H).

^{13}C NMR (151 MHz, CD_2Cl_2) δ 172.26, 170.23, 155.38, 154.76, 144.82, 141.20, 131.58, 130.77, 128.16, 122.16, 115.73, 52.71, 37.38, 37.29, 24.12, 16.65, 14.59.

HRMS $[M+Na]^+$ calcd. 520.21896 for $C_{26}H_{30}BF_2N_3O_4Na^+$, found 520.21886.

5.2.1.2 pNP-Tyr(OMe)-BODIPY (2)

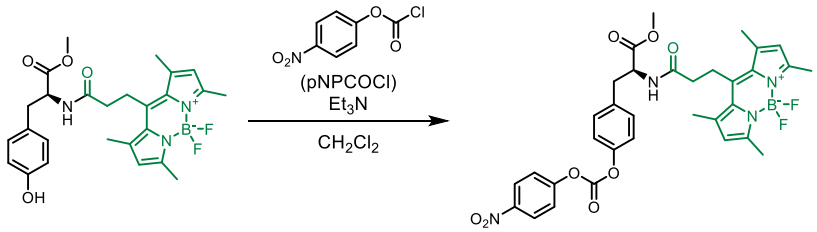

1
$C_{26}H_{30}BF_2N_3O_4$
497.35

2
$C_{33}H_{33}BF_2N_4O_8$
662.45

The synthesis was carried out following the procedure[73] described in literature with modifications.

To a solution of **1** (22.2 mg, 44.7 µmol) in CH_2Cl_2 (3 mL) was added a solution of pNPCOCl (9.9 mg, 49 µmol) in CH_2Cl_2 (1 mL), Et_3N (14.9 µL, 11 mg, 107 µmol) and heated to reflux for 1 h, until full conversion was monitored by TLC. Purification by preparative NP-HPLC (hexane/EE gradient elution) gave the desired product **2** as an orange solid (27.2 mg, 92 %).

Rf.: 0.23 (PE:EE / 1:1)

^{1}H NMR (600 MHz, CD_2Cl_2) δ 8.35 – 8.27 (m, 2H), 7.51 – 7.46 (m, 2H), 7.24 – 7.19 (m, 2H), 7.19 – 7.14 (m, 2H), 6.09 (s, 2H), 5.98 (d, *J* = 7.7 Hz, 1H), 4.88 (dt, *J* = 7.8, 6.0 Hz, 1H), 3.74 (s, 3H), 3.33 – 3.24 (m, 2H), 3.21 (dd, *J* = 14.0, 5.7 Hz, 1H), 3.08 (dd, *J* = 14.0, 6.2 Hz, 1H), 2.53 – 2.38 (m, 14H).

^{13}C NMR (151 MHz, CD_2Cl_2) δ 171.98, 170.22, 155.65, 154.79, 151.50, 150.20, 146.08, 144.78, 141.17, 135.20, 131.58, 130.92, 125.75, 122.25, 122.16, 121.31, 52.83, 37.57, 37.41, 24.10, 16.66, 14.59.

HRMS $[M+Na]^+$ calcd. 685.22517 for $C_{33}H_{33}BF_2N_4O_8Na^+$, found 685.22399.

5.2.1.3 rTCO-SIL1-Tyr(OMe)-BODIPY (3)

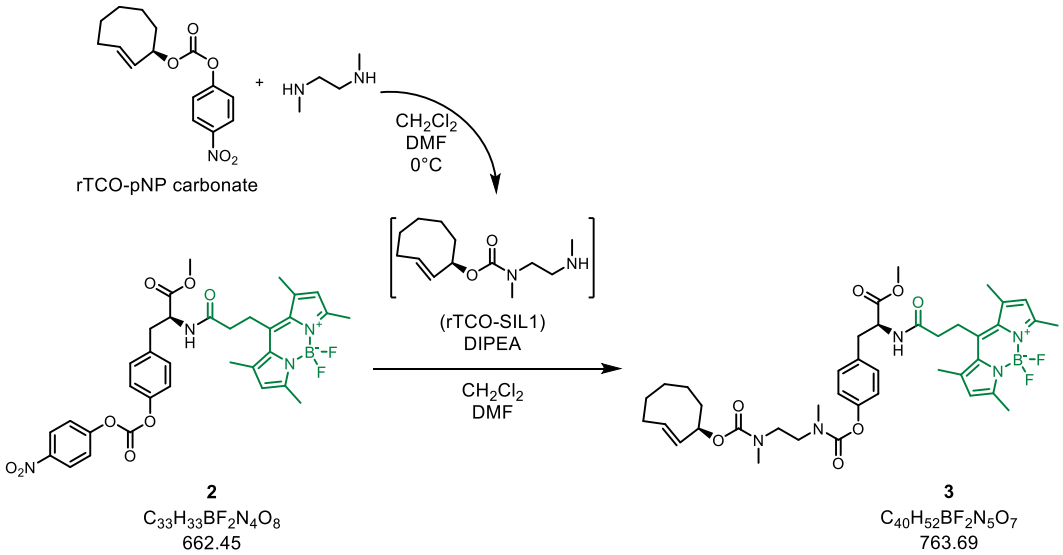

The synthesis was carried out following the procedure[74] described in literature with modifications.

A solution of rTCO-pNP carbonate[25] (axial, 18.7 mg, 64.3 µmol) in CH_2Cl_2 (4 mL) was added via syringe pump (30 µL/min) to a solution of *N*,*N'*-dimethylethane-1,2-diamine (70.0 µL, 56.7 mg, 643 µmol) in CH_2Cl_2 (1.2 mL) and DMF (0.4 mL) at 0 °C. After full addition within 2 h the solution was stirred for additional 1 h at 0 °C. Excess of free amine was then removed on the high vacuum for 3 h leaving crude intermediate. The resulting crystallites were redissolved in CH_2Cl_2 (600 µL) and added to a solution of **2** (21.3 mg, 32.2 µmol) in DMF (300 µL) at rt. Followed by addition of DIPEA (60µL) after 15 min, crude product was obtained after 2 h of stirring. Purification by preparative NP-HPLC (hexane/EE gradient elution) gave the desired product **3** as an orange solid (18.0 mg, 74 %).

^{1}H NMR (600 MHz, CD_2Cl_2, rotamers) δ 7.10 – 7.04 (m, 2H), 7.04 – 6.97 (m, 2H), 6.09 (s, 2H), 6.00 (s, 1H), 5.85 – 5.69 (m, 1H), 5.59 – 5.45 (m, 1H), 4.85 (dt, *J* = 7.4, 5.8 Hz, 1H), 3.73 (s, 3H), 3.67 – 3.38 (m, 4H), 3.35 – 3.20 (m, 2H), 3.15 (dd, *J* = 14.0, 5.7 Hz, 1H), 3.12 – 2.91 (m, 7H), 2.53 – 2.38 (m, 15H), 2.10 – 1.59 (m, 6H), 1.52 – 1.42 (m, 1H), 1.14 – 0.99 (m, 1H), 0.86 – 0.72 (m, 1H).

^{13}C NMR (151 MHz, CD_2Cl_2, rotamers) δ 172.08, 170.21, 170.19, 155.97, 155.85, 155.57, 155.06, 154.89, 154.72, 151.15, 151.10, 151.02, 144.88, 141.23, 133.39, 133.28, 133.15, 132.07, 131.96, 131.59, 130.39, 130.31, 122.42, 122.36, 122.31, 122.23, 122.13, 74.95, 74.87, 74.73, 74.62, 53.57, 52.74, 47.82, 47.66, 47.41, 47.32, 47.16, 47.11, 46.68, 46.54, 41.14, 41.02, 37.46, 37.43, 37.32, 36.40, 36.34, 36.21, 36.13, 35.62, 35.54, 35.50, 35.45, 35.27, 35.23, 34.97, 34.54, 32.31, 30.08, 30.04, 29.75, 29.70, 29.43, 29.35, 24.71, 24.53, 24.14, 23.08, 16.67, 14.27.

HRMS $[M+Na]^+$ calcd. 786.38201 for $C_{40}H_{52}BF_2N_5O_7Na^+$, found 786.38128.

5.2.1.4 rTCO-SIL1-Tyr(mPEG7)-BODIPY (4)

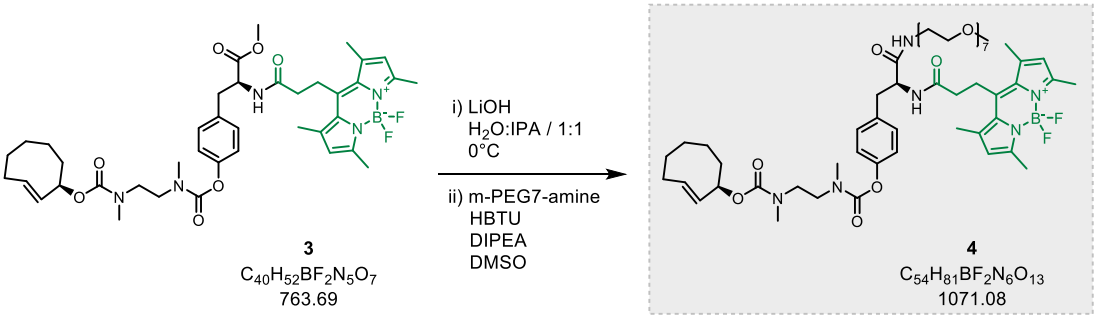

A saturated solution of LiOH in H_2O/IPA (5 mL, H_2O:IPA / 1:1) was added to **3** (6.18 mg, 8,1 µmol) and stirred for 1 h at 0 °C. LCMS indicated complete conversion to the desired free acid. The clear solution was drained onto IPA (20 mL), syringe filtrated and concentrated. The residue redissolved in H_2O again, was eluted through a Pasteur pipette filled with cationic exchange resin (Amberlite R120, 5 mL, 1 mL/min) and concentrated again, yielding an orange crude intermediate (8.1 mg), which was used without further purification. To a solution of crude intermediate (4.0 mg) in DMSO (0.5 mL) HBTU (3.0 mg, 7.9 µmol), DIPEA (4.6 µL, 3.4 mg, 26.3 µmol) and m-PEG7-amine (5.0 µL, 5.0 mg, 15 µmol, gravimetric determined due to manufacturer´s non-specified density) were added and stirred for 1 h at rt. LCMS indicated complete conversion to the desired product. Purification by preparative RP-HPLC (H_2O/MeCN gradient elution, 0.1 % formic acid) gave the desired product **4** as a red-brown solid (3.6 mg, 85 %).

^{1}H NMR (600 MHz, CD_2Cl_2, rotamers) δ 7.20 – 7.11 (m, 2H), 7.04 – 6.97 (m, 2H), 6.62 – 6.37 (m, 1H), 6.09 (s, 2H), 5.85 – 5.69 (m, 0.5H), 5.59 – 5.45 (m, 0.5H), 4.70 – 4.60 (m, 1H), 3.64 – 3.53 (m, 21H), 3.52 – 3.41 (m, 6H), 3.40 – 3.35 (m, 2H), 3.32 (s, 3H), 3.29 – 3.17 (m, 1H), 3.13 – 3.05 (m, 2H), 3.03 – 2.96 (m, 4H), 2.95 – 2.90 (m, 1H), 2.46 (s, 5H), 2.42 (s, 6H), 2.10 – 1.90 (m, 5H), 1.89-1.78 (m, 1H), 1.78 – 1.64 (m, 4H), 1.54 – 1.44 (m, 1H), 1.14 – 1.04 (m, 1H), 0.86 – 0.80 (m, 1H).

^{13}C NMR (151 MHz, CD_2Cl_2, rotamers) δ 170.70, 170.22, 154.82, 154.64, 150.90, 145.12, 141.28, 132.08, 131.99, 131.61, 130.55, 130.29, 130.12, 122.26, 122.20,

122.10, 114.15, 107.36, 74.95, 74.88, 74.73, 74.63, 72.25, 70.82, 70.72, 70.58, 69.83, 59.00, 54.67, 54.62, 54.57, 47.85, 47.68, 47.44, 47.20, 47.13, 46.70, 46.57, 41.15, 41.06, 40.63, 39.75, 39.71, 38.39, 38.31, 37.83, 37.78, 37.73, 37.68, 37.44, 37.37, 37.31, 37.02, 36.67, 36.62, 36.40, 36.22, 36.09, 34.02, 33.85, 33.55, 33.14, 33.08, 32.32, 30.52, 30.46, 30.41, 30.32, 30.17, 30.08, 30.05, 29.90, 29.83, 29.75, 29.71, 29.65, 29.59, 29.54, 29.44, 29.37, 29.32, 28.36, 28.27, 27.84, 27.55, 27.53, 27.44, 27.02, 26.88, 25.88, 25.54, 24.81, 24.73, 24.54, 24.23, 23.56, 23.09, 22.84, 22.78, 19.90, 19.84, 19.37, 16.70, 14.59, 14.37, 14.34, 14.28, 12.61, 11.57, 7.65, 7.62.

HRMS $[M+Na]^+$ calcd. 1093.58149 for $C_{54}H_{81}BF_2N_6O_{13}Na^+$, found 1093.58223.

5.2.2 Target compound for primary alcohol release

5.2.2.1 Ser(OMe)-BODIPY (5)

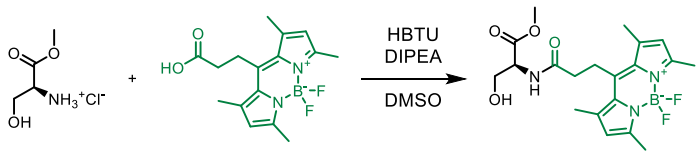

BODIPY-acid
$C_{16}H_{19}BF_2N_2O_2$
320.15

5
$C_{20}H_{26}BF_2N_3O_4$
421.25

To a solution of BODIPY-acid (28 mg, 87.5 µmol) in DMSO (4 mL) *L*-serine methyl ester hydrochloride (27.2 mg, 175 µmol), HBTU (35.5 mg, 93.7 µmol) and DIPEA (53.1 µL, 40.3 mg, 312 µmol) were added and stirred for 1 h at rt. LCMS indicated complete conversion to the desired product. Purification by preparative RP-HPLC (H_2O/MeCN gradient elution, 0.1 % formic acid) gave the desired product **5** as red solid (32.5 mg, 88 %).

^{1}H NMR (600 MHz, CD_2Cl_2) δ 6.35 (d, *J* = 7.7 Hz, 1H), 6.11 (s, 2H), 4.61 (dt, *J* = 7.6, 3.4 Hz, 1H), 3.92 (ddd, *J* = 11.1, 5.0, 3.5 Hz, 1H), 3.74 (s, 3H), 3.65 (ddd, *J* = 11.2, 5.6, 3.3 Hz, 1H), 3.41 (ddd, *J* = 13.7, 10.5, 6.8 Hz, 1H), 3.31 (ddd, *J* = 13.7, 10.6, 5.0 Hz, 1H), 2.61 (ddd, *J* = 15.3, 10.5, 5.0 Hz, 1H), 2.56 – 2.49 (m, 1H), 2.49 – 2.43 (m, 12H), 2.36 (s, 1H).

^{13}C NMR (151 MHz, CD_2Cl_2) δ 171.11, 170.87, 154.80, 144.88, 141.48, 131.71, 122.27, 63.53, 54.88, 52.99, 37.86, 24.16, 16.68, 14.60.

HRMS $[M+Na]^+$ calcd. 444.18766 for $C_{20}H_{26}BF_2N_3O_4Na^+$, found 444.18699.

5.2.2.2 Ser(mPEG7)-BODIPY (6)

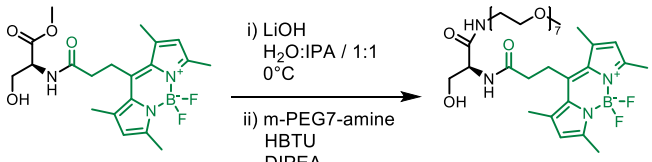

5
$C_{20}H_{26}BF_2N_3O_4$
421.25

6
$C_{22}H_{31}BF_2N_4O_4$
728.64

A saturated solution of LiOH in H_2O/IPA (4.9 mL, H_2O:IPA / 1:1) was added to **5** (28.19 mg, 66,9 µmol) and stirred for 5 min at rt. LCMS indicated complete conversion to the desired free acid. The clear solution was drained onto a mixture of cationic exchange resin (Amberlite R120, 20 mL) in H_2O/IPA (80 mL, H_2O:IPA / 1:1) and stirred for additional 1.5 h. The solution was syringe filtrated and concentrated yielding an orange crude intermediate, which was used without further purification. To a solution of crude intermediate in DMSO (4.3 mL) m-PEG7-amine (63.6 µL, 63.6 mg, 187 µmol), HBTU (38.1 mg, 100 µmol) and DIPEA (56.9 µL, 43.3 mg, 335 µmol) were added and stirred for 1 h at rt. LCMS indicated complete conversion to the desired product. Purification by preparative RP-HPLC (H_2O/MeCN gradient elution, 0.1% formic acid) gave the desired product **6** as a red solid (7.8 mg, 16 %).

^{1}H NMR (600 MHz, CD_2Cl2) δ 7.15 (t, *J* = 5.6 Hz, 1H), 6.91 (d, *J* = 7.2 Hz, 1H), 6.09 (s, 2H), 4.41 (ddd, *J* = 7.1, 5.7, 3.9 Hz, 1H), 3.90 (dd, *J* = 10.7, 4.0 Hz, 1H), 3.70 – 3.27 (m, 34H), 2.70 – 2.26 (m, 14H).

^{13}C NMR (151 MHz, CD_2Cl_2) δ 171.12, 170.84, 154.66, 145.19, 141.30, 131.65, 122.12, 72.21, 70.83, 70.76, 70.72, 70.68, 70.52, 69.72, 63.24, 58.99, 54.87, 39.66, 37.30, 30.07, 24.13, 16.69, 14.58.

HRMS $[M+H]^+$ calcd. 729.40521 for $C_{34}H_{56}BF_2N_4O_{10}^+$, found 729.40626.

5.2.2.3 rTCO-SIL1-Ser(mPEG7)-BODIPY (7)

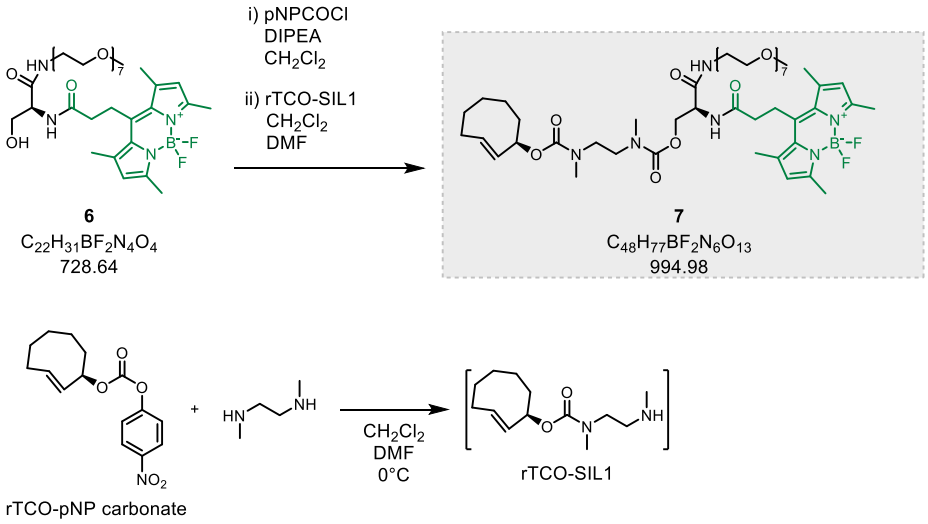

The synthesis was carried out following the procedure[73] described in literature with modifications.

i) DIPEA (0.4 µL, 0.5 mg, 4 µmol) was added to a solution of **6** (6.9 mg, 9.5 µmol) and pNPCOCl (9.5 mg, 47.4 µmol) in CH_2Cl_2 (200 µL) and stirred at 35 °C. Within intervals of 20 min DIPEA (0.4 µL, 0.5 mg, 4 µmol) was added 3x. pNPCOCl (9.5 mg, 47.4 µmol) was added again followed by addition of DIPEA (0.4 µL, 0.5 mg, 4 µmol) in intervals of 20 min (4x). After full conversion, verified via LCMS, the reaction was quenched using saturated NH_4Cl solution, extracted with CH_2Cl_2 (3x) and concentrated to give a red crude product (23 mg).

HRMS $[M+H]^+$ calcd. 894.41141 for $C_{41}H_{59}BF_2N_5O_{14}^+$, found 894.41217.

The synthesis was carried out following the procedure[74] described in literature with modifications.

ii) A solution of rTCO-pNP carbonate (6.7 mg, 22.9 µmol) in CH_2Cl_2 (1.3 mL) was added via syringe pump (30 µL/min) to a solution of *N*,*N'*-dimethylethane-1,2-diamine (24.9 µL, 20.2 mg, 229 µmol) in CH_2Cl_2 (0.4 mL) and DMF (0.14 mL) at 0 °C.

After full addition within 40 min the solution was stirred for additional 1 h at 0 °C. Excess of free amine was then removed on the high vacuum for 3 h leaving crude intermediate. The resulting crystallites were then redissolved in CH_2Cl_2 (400 µL) and added to a solution of crude pNP-Intermediate (10.3 mg) in DMF (200 µL) at rt. After full conversion within 30 min, verified via LCMS, the solvents were removed. Purification by preparative NP-HPLC (CH_2Cl_2/MeOH gradient elution) gave the desired product **7** as a red solid (1.4 mg, 31 %).

^{1}H NMR (600 MHz, CD_2Cl_2, rotamers) δ 8.00 – 7.87 (m, 1H), 6.89 – 6.73 (m, 1H), 6.10 (s, 2H), 5.83 – 5.64 (m, 1H), 5.62 – 5.54 (m, 0.5H), 5.36 – 5.34 (m, 1H), 5.22 – 5.16 (m, 0.5H), 5.00 – 4.86 (m, 1H), 4.79 – 4.72 (m, 1H), 4.65 – 4.56 (m, 1H), 4.23 – 4.13 (m, 1H), 3.55 – 3.52 (m,5H), 3.51 – 3.44 (m, 4H), 3.41 – 3.35 (m, 3H), 3.33 (s, 3H), 3.32 – 3.27 (m, 2H), 3.21 – 3.05 (m, 2H), 2.95 (d, *J* = 2.2 Hz, 3H), 2.87 (d, *J* = 5.2 Hz, 3H), 2.75 – 2.61 (m, 2H), 2.49 – 2.44 (m, 14H), 2.11 – 1.69 (m, 8H), 1.59 – 1.52 (m, 10H), 1.33 – 1.20 (m, 3H).

^{13}C NMR (151 MHz, CD_2Cl_2, rotamers) δ 171.46, 171.38, 169.72, 156.49, 155.64, 155.62, 145.91, 132.25, 131.85, 131.53, 131.30, 130.29, 126.44, 125.37, 122.23, 122.09, 116.06, 75.60, 75.54, 72.25, 70.86, 70.74, 70.56, 69.99, 65.34, 59.01, 53.24, 53.18, 47.44, 47.36, 46.64, 46.61, 41.12, 40.52, 40.10, 39.78, 39.69, 36.74, 36.55, 36.47, 36.37, 36.20, 36.11, 35.79, 34.86, 34.01, 33.43, 32.32, 30.16, 30.08, 30.04, 29.99, 29.90, 29.85, 29.75, 29.71, 29.65, 29.59, 29.53, 29.44, 29.04, 28.88, 27.55, 27.13, 27.01, 26.80, 26.32, 25.87, 25.77, 25.15, 24.58, 24.37, 23.93, 23.86, 23.09, 16.68, 16.59, 14.61, 14.28.

HRMS $[M+Na]^+$ calcd. 1017.55019 for $C_{48}H_{77}BF_2N_6O_{13}Na^+$, found 1017.55206.

5.2.3 Target compound for primary amine release

5.2.3.1 pNP-SIL2-TBDMS (8)

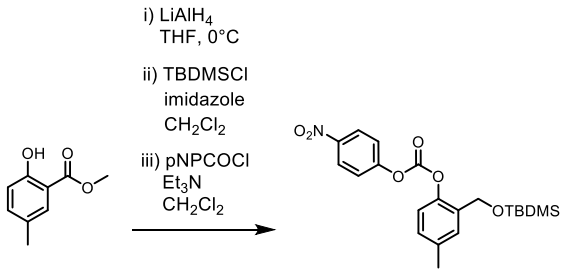

$C_9H_{10}O_3$
166.18

8
$C_{21}H_{27}NO_6Si$
417.53

The synthesis was carried out following the procedure[75] described in literature with modifications.

i) Methyl 5-methylsalicylate (3.55 g, 21,4 mmol) dissolved in THF (15 mL) was slowly added to a suspension of $LiAlH_4$ in THF (10 mL) at 0 °C. After complete addition, the temperature was raised to reflux for 2 h, until full conversion could be obtained by TLC. The Reaction mixture was acidified to pH 1 with 1 N HCl and extracted with Et_2O (3x). The organic phases were combined, dried over Na_2SO_4 and concentrated to give an off-white solid (2.88 g, 98 %), which was used without further purification.

HRMS $[M+H]^+$ calcd. 139.07536 for $C_8H_{11}O_2^+$, found 139.07523.

The synthesis was carried out following the procedure[76] described in literature with modifications.

ii) To a 0 °C cooled mixture of crude 5-methyl salicyl alcohol (1.50 g, 10.9 mmol) and imidazole (2.22 g, 32.6 mmol) in CH_2Cl_2, TBDMSCl (2.45 g, 16.3 mmol) dissolved in CH_2Cl_2 (6 mL) was added within 1 h and GCMS indicated complete conversion to the desired product. The reaction was quenched by addition of H_2O and extracted with CH_2Cl_2 (3x), the combined organic phases were dried over Na_2SO_4 and concentrated to give a yellow oil (3.31 g, 121 %), which was used without further purification.

HRMS $[M+Na]^+$ calcd. 275.14378 for $C_{14}H_{24}O_2SiNa^+$, found 275.14352.

The synthesis was carried out following the procedure[73] described in literature with modifications.

iii) A mixture of crude TBDMS-intermediate (2 g, 7.9 mmol), pNPCOCl (7.76 g, 8.7 mmol) and Et_3N (1.92 g, 2.64 mL, 19,0 mmol) dissolved in CH_2Cl_2 (100 mL) was heated to reflux. Upon heating the solution turned orange and full conversion, monitored via TLC, was obtained after 5 h. After cooling to rt, the organic phase was extracted with saturated $NaHCO_3$ (100 mL, 3x) and the aqueous phase re-extracted with CH_2Cl_2. The combined organic phases were dried over Na_2SO_4 and concentrated yielding a yellow crude solid which was purified by flash chromatography (PE/CH_2Cl_2 gradient elution, 1500 g silica gel) to give the desired product **8** as a white solid (1.50 g, 45 %, overall yield over 3 steps: 54 %).

Rf.: 0.44 (PE:EE / 9:1).

^{1}H NMR (400 MHz, CD_2Cl_2) δ 8.35 – 8.27 (m, 2H), 7.54 – 7.45 (m, 2H), 7.34 (s, 1H), 7.19 – 7.09 (m, 2H), 4.75 (s, 2H), 2.38 (s, 3H), 0.94 (s, 9H), 0.12 (s, 6H).

^{13}C NMR (101 MHz, CD_2Cl_2) δ 155.85, 151.35, 146.35, 146.01, 137.24, 132.91, 129.54, 129.21, 125.74, 122.15, 121.33, 60.79, 26.06, 21.15, 18.68, -5.22.

HRMS $[M+H]^+$ calcd. 418.16804 for $C_{21}H_{28}NO_6Si^+$, found 418.16767.

5.2.3.2 rTCO-SIL1-SIL2-TBDMS (9)

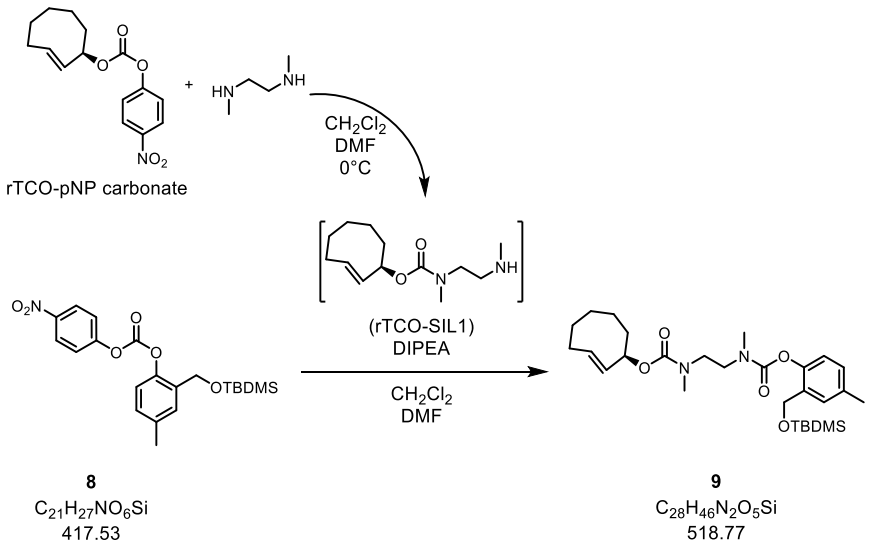

The synthesis was carried out following the procedure[74] described in literature with modifications.

A solution of rTCO-pNP carbonate (20 mg, 68.7 µmol) in CH_2Cl_2 (4 mL) was added via syringe pump (30 µL/min) to a solution of *N*,*N*'-Dimethylethane-1,2-diamine (60.5 mg, 79.6 µL, 0.69 mmol) in CH_2Cl_2 (1.2 mL) and DMF (0.4 mL) at 0 °C. After full addition within 2 h the solution was stirred for additional 1 h at 0 °C. Excess of free amine was then removed on the high vacuum for 3 h leaving crude intermediate. The resulting crystallites were then redissolved in DMF (0.3 mL) cooled to 0 °C and a solution of **8** (43 mg, 0.1 mmol) in CH_2Cl_2 (0.6 mL) was added. Followed by addition of DIPEA (60 µL) after 15 min, complete conversion to the desired product was indicated via LCMS after 2 h of stirring. Purification by preparative NP-HPLC (hexane/EtOAc gradient elution) gave the desired product **9** as colourless oil (35.1 mg, 99 %).

^{1}H NMR (600 MHz, CD_2Cl_2,rotamers) δ 7.29 (s, 1H), 7.09 – 7.01 (m, 1H), 6.94 – 6.86 (m, 1H), 5.87 – 5.70 (m, 1H), 5.60 – 5.48 (m, 1H), 5.38 – 5.33 (m, 1H), 4.70 – 4.59 (m, 2H), 3.68 – 3.39 (m, 4H), 3.15 – 2.90 (m, 6H), 2.52 – 2.39 (m, 1H), 2.34 (s, 3H), 2.11 – 1.46 (m, 7H), 1.16 – 0.98 (m, 1H), 0.94 (s, 9H), 0.86 – 0.71 (m, 1H), 0.09 (s, 6H).

^{13}C NMR (151 MHz, CD_2Cl_2, rotamers) δ 155.91, 155.82, 155.52, 154.89, 154.75, 154.64, 146.61, 146.56, 135.66, 135.48, 135.37, 133.76, 133.68, 133.54, 132.06, 131.98, 131.94, 128.56, 128.50, 128.43, 122.36, 122.30, 122.19, 74.92, 74.85, 74.75, 74.63, 60.57, 60.47, 60.44, 47.99, 47.74, 47.68, 47.36, 47.32, 47.24, 46.77, 46.73, 41.18, 41.14, 41.11, 36.39, 36.30, 36.21, 36.13, 35.72, 35.66, 35.59, 35.41, 35.06, 34.76, 29.46, 29.38, 26.06, 24.71, 24.54, 21.12, 18.64, -5.26.

HRMS $[M+H]^+$ calcd. 519.32488 for $C_{28}H_{47}N_2O_5Si^+$, found 519.32484.

5.2.3.3 rTCO-SIL1-SIL2-pNP (10)

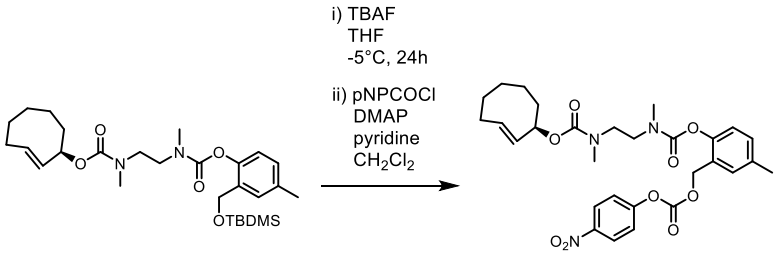

9
$C_{28}H_{46}N_2O_5Si$
518.77

10
$C_{29}H_{35}N_3O_9$
569.61

The synthesis was carried out following the procedure[77] described in literature with modifications.

i) To a solution of **9** (35.11 mg, 67.8 µmol) in THF (744 µL) at -5°C was added a K_2HPO_4 buffered solution of TBAF in THF (22.6 µL, 74.5 µmol, 3.3 M) and stirred for 24 h. The mixture was quenched with saturated NH_4Cl solution (3 mL) and extracted with CH_2Cl_2 (3x). The combined organic phases were dried over Na_2SO_4 and concentrated to give a colourless oil, which was used without further purification.

HRMS $[M+H]^+$ calcd. 405.23840 for $C_{22}H_{33}N_2O_5^+$, found 405.23911.

ii) A solution of DMAP (4.13 mg, 33.8 µmol) in CH_2Cl_2 (750 µL), pyridine (18.7 mg, 19.2 µL) and a solution of pNPCOCl (17.1 mg, 84.6 µmol) in CH_2Cl_2 (750 µL) were added to the crude intermediate and stirred for 3 h. LCMS indicated complete conversion of the primary alcohol to the desired product. The mixture was quenched with saturated NH_4Cl solution (3 mL) and extracted with CH_2Cl_2 (3x). The combined organic phases were concentrated and purification by preparative NP-HPLC (hexane/EtOAc gradient elution) gave the desired product **10** as colourless oil (15.5 mg, 40 %, 100 % b.r.s.m. yield).

^{1}H NMR (600 MHz, CD_2Cl_2, rotamers) δ 8.26 (dd, *J* = 9.1, 1.9 Hz, 2H), 7.43 – 7.35 (m, 2H), 7.32 – 7.26 (m, 1H), 7.26 – 7.17 (m, 1H), 7.07 – 7.00 (m, 1H), 5.84 – 5.71 (m, 1H), 5.58 – 5.48 (m, 1H), 5.33 (s, 1H), 5.28 – 5.21 (m, 2H), 3.70 – 3.39 (m, 4H), 3.17 –

2.90 (m, 6H), 2.46 – 2.39 (m, 1H), 2.37 (s, 3H), 2.09 – 1.45 (m, 7H), 1.13 – 1.03 (m, 1H), 0.85 (s, 1H).

^{13}C NMR (151 MHz, CD_2Cl_2, rotamers) δ 156.02, 155.98, 155.88, 155.55, 154.86, 154.74, 154.65, 152.78, 152.75, 152.53, 151.93, 148.17, 148.13, 148.07, 145.79, 136.46, 136.23, 136.00, 135.86, 135.72, 135.53, 134.35, 132.09, 132.03, 131.95, 131.92, 131.18, 131.16, 131.10, 131.05, 130.99, 130.96, 127.20, 127.09, 126.95, 126.93, 125.59, 125.06, 124.92, 124.74, 123.26, 123.19, 123.17, 123.09, 122.33, 122.29, 74.96, 74.88, 74.76, 74.65, 66.68, 66.62, 47.95, 47.76, 47.57, 47.42, 47.33, 47.12, 46.64, 41.16, 41.14, 41.07, 37.78, 37.74, 37.71, 37.44, 36.45, 36.39, 36.30, 36.20, 36.12, 35.78, 35.64, 35.62, 35.55, 35.40, 35.33, 35.28, 34.99, 34.59, 34.52, 34.01, 32.32, 31.58, 31.51, 30.46, 30.44, 29.76, 29.44, 29.36, 24.71, 24.52, 23.09, 20.92, 14.28.

HRMS $[M+H]^+$ calcd. 570.24461 for $C_{29}H_{36}N_3O_9^+$, found 570.24535.

5.2.3.4 BocLys(mPEG7)-BODIPY (11)

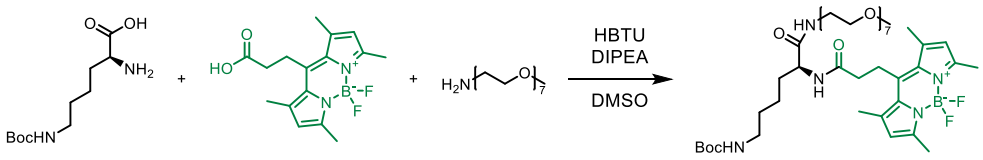

DIPEA (26.6 µL, 20.2 mg, 156 µmol) was added to a solution of BODIPY-acid (10 mg, 31.2 µmol) and HBTU (13.03 mg, 34.4 µmol) in DMSO (0.5 mL) and stirred for 20 min at rt. *N*$^{\varepsilon}$-Boc-*L*-lysine (8.5 mg, 34 µmol), suspended in DMSO (0.5 mL) was added slowly and the solution was stirred for 1 h. LCMS revealed complete consumption of BODIPY-acid and the formation of BocLys-BODIPY adduct. Again HBTU (17.8 mg, 46.9 µmol) dissolved in DMSO (0.4 mL) was added, the mixture stirred for 10 min followed by addition of m-PEG7-amine (21.2 µL, 21.2 mg, 62.5 µmol) and stirred for 1 h. LCMS revealed complete consumption of the BocLys-BODIPY adduct and the formation of the desired product as major compound. Purification by preparative RP-HPLC (H_2O/MeCN gradient elution, 0.1 % formic acid) gave the desired product **11** as a red solid (10.1 mg, 37 %).

^{1}H NMR (600 MHz, CD_2Cl_2) δ 7.51 – 7.15 (m, 1H), 6.83 – 6.70 (m, 1H), 6.68 – 6.53 (m, 1H), 6.10 (s, 2H), 4.86 – 4.76 (m, 1H), 4.42 – 4.29 (m, 1H), 3.71 – 3.64 (m, 2H), 3.63 – 3.55 (m, 22H), 3.54 – 3.48 (m, 5H), 3.43 – 3.38 (m, 2H), 3.71 – 3.64 (m, 2H), 3.35 – 3.29 (m, 5H), 3,19 – 3.10 (m, 4H), 2.46 (d, *J* = 6.8Hz, 12H), 1.74 (s, 9H).

^{13}C NMR (151 MHz, CD_2Cl_2) δ 171.91, 170.66, 156.38, 154.63, 145.24, 141.25, 131.63, 122.11, 79.07, 72.17, 70.81, 70.79, 70.75, 70.73, 70.66, 70.52, 70.01, 59.00, 55.66, 47.43, 43.69, 40.38, 39.61, 37.36, 32.70, 30.07, 29.92, 28.51, 24.22, 22.83, 18.76, 17.40, 16.67, 14.59, 12.75, 8.93.

HRMS $[M+H]^+$ calcd. 870.52057 for $C_{42}H_{71}BF_2N_5O_{11}^+$, found 870.52015.

5.2.3.5 rTCO-SIL1-SIL2-Lys(mPEG7)-BODIPY (12)

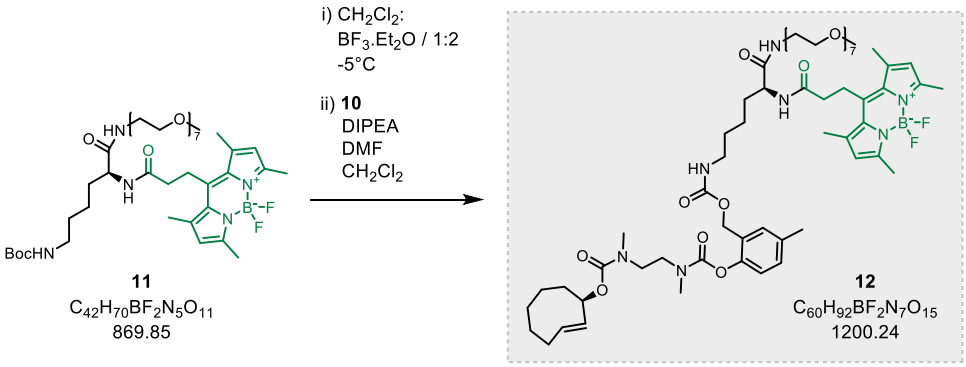

i) To a solution of **11** (9.13 mg, 10.5 µmol) in CH_2Cl_2 (250 µL) at -5°C was added $BF_3.Et_2O$ (500 µL) and stirred for 1.5 h. LCMS revealed formation of the desired primary amine as major compound. The mixture was quenched with saturated $NaHCO_3$ / ice and extracted with CH_2Cl_2 (3x). The combined organic phases were concentrated to give a red solid (10.5 mg), which was used without further purification.

HRMS $[M+H]^+$ calcd. 770.46814 for $C_{37}H_{63}BF_2N_5O_9^+$, found 770.46937.

ii) Deprotected intermediate of **11** (21.8 mg) dissolved in CH_2Cl_2 (600 µL) was added to a solution of **10** (7.40 mg, 13.0 µmol) in DMF (300 µL) and stirred for 1 h. After addition of DIPEA (90 µL) the mixture was stirred for further 2.5 h and concentrated. LCMS indicated conversion to the desired product. Purification by preparative NP-HPLC (CH_2Cl_2/MeOH gradient elution) gave the desired product **12** as an orange solid (4.1 mg, 26 %).

^{1}H NMR (600 MHz, CD_2Cl_2, rotamers) δ 7.24 – 7.02 (m, 2H), 6.90 (d, *J* = 6.8Hz, 1H), 6.76 – 6.50 (m, 2H), 6.08 (s, 2H), 5.83 – 5.69 (m, 1H), 5.59 – 5.43 (m, 1H), 5.02 – 5.87 (m, 2H), 4.41 – 4.30 (m, 1H), 3.63 – 3.55 (m, 22H), 3.52 – 3.48 (m, 5H), 3.41 – 3.35 (m, 2H), 3.31 – 3.24 (m, 2H), 3.17 – 3.04 (m, 4H), 3.03 – 2.86 (m, 5H), 2.52 – 2.41 (m, 14H), 2.11 - 1.42 (m, 22H), 1.33 – 1.20 (m, 4H).

^{13}C NMR (151 MHz, CD_2Cl_2, rotamers) δ 170.71, 156.73, 156.00, 154.89, 154.68, 154.60, 148.19, 147.91, 145.29, 141.24, 135.91, 135.53, 132.28, 132.09, 131.92, 131.76, 131.62, 131.28, 131.00, 130.93, 130.49, 130.28, 130.11, 129.91, 129.11, 125.37, 122.93, 122.08, 75.02, 74.90, 74.73, 72.21, 70.88, 70.80, 70.77, 70.67, 70.54, 69.97, 62.47, 62.34, 62.09, 61.78, 59.00, 53.84, 47.77, 47.67, 47.46, 47.23, 47.12, 46.74, 46.51, 41.13, 41.08, 40.82, 40.78, 40.67, 39.60, 37.32, 37.29, 36.38, 36.29, 36.20, 36.11, 35.63, 35.55, 35.29, 35.13, 34.54, 32.65, 32.53, 32.45, 32.32, 32.30, 31.52, 30.12, 30.09, 30.05, 30.01, 29.88, 29.76, 29.71, 29.67, 29.43, 29.41, 27.55, 26.80, 24.74, 24.70, 24.50, 24.26, 23.58, 23.09, 22.66, 20.86, 16.67, 14.61, 14.59, 14.58, 14.28.

HRMS $[M+H]^+$ calcd. 1200.67853 for $C_{60}H_{93}BF_2N_7O_{15}^+$, found 1200.67916.

Bibliography

1. Dube, D. H. & Bertozzi, C. R. Metabolic oligosaccharide engineering as a tool for glycobiology. *Curr. Opin. Chem. Biol.* **7**, 616–625 (2003).

2. Sletten, E. M. & Bertozzi, C. R. From Mechanism to Mouse: A Tale of Two Bioorthogonal Reactions. *Acc. Chem. Res.* **44**, 666–676 (2011).

3. Prescher, J. A., Dube, D. H. & Bertozzi, C. R. Chemical remodelling of cell surfaces in living animals. *Nature* **430**, 873–877 (2004).

4. Sletten, E. M. & Bertozzi, C. R. Bioorthogonal Chemistry: Fishing for Selectivity in a Sea of Functionality. *Angew. Chemie Int. Ed.* **48**, 6974–6998 (2009).

5. McKay, C. S. & Finn, M. G. Click Chemistry in Complex Mixtures: Bioorthogonal Bioconjugation. *Chem. Biol.* **21**, 1075–1101 (2014).

6. Campbell-Verduyn, L. S. *et al.* Strain-Promoted Copper-Free “Click” Chemistry for 18F Radiolabeling of Bombesin. *Angew. Chemie Int. Ed.* **50**, 11117–11120 (2011).

7. Lang, K. & Chin, J. W. Cellular Incorporation of Unnatural Amino Acids and Bioorthogonal Labeling of Proteins. *Chem. Rev.* **114**, 4764–4806 (2014).

8. Li, Z. *et al.* Tetrazine–trans-cyclooctene ligation for the rapid construction of 18F labeled probes. *Chem. Commun.* **46**, 8043 (2010).

9. Haun, J. B., Devaraj, N. K., Hilderbrand, S. A., Lee, H. & Weissleder, R. Bioorthogonal chemistry amplifies nanoparticle binding and enhances the sensitivity of cell detection. *Nat. Nanotechnol.* **5**, 660–665 (2010).

10. Devaraj, N. K. & Weissleder, R. Biomedical Applications of Tetrazine Cycloadditions. *Acc. Chem. Res.* **44**, 816–827 (2011).

11. Wu, H., Cisneros, B. T., Cole, C. M. & Devaraj, N. K. Bioorthogonal Tetrazine-Mediated Transfer Reactions Facilitate Reaction Turnover in Nucleic Acid-Templated Detection of MicroRNA. *J. Am. Chem. Soc.* **136**, 17942–17945 (2014).

12. Wu, H., Alexander, S. C., Jin, S. & Devaraj, N. K. A Bioorthogonal Near-Infrared Fluorogenic Probe for mRNA Detection. *J. Am. Chem. Soc.* **138**, 11429–11432 (2016).

13. Baskin, J. M. *et al.* Copper-free click chemistry for dynamic in vivo imaging. *Proc. Natl. Acad. Sci.* **104**, 16793–16797 (2007).

14. Devaraj, N. K., Weissleder, R. & Hilderbrand, S. a. Tetrazine-Based

Cycloadditions: Application to Pretargeted Live Cell Imaging. *Bioconjug. Chem.* **19**, 2297–2299 (2008).

15. Laughlin, S. T., Baskin, J. M., Amacher, S. L. & Bertozzi, C. R. In Vivo Imaging of Membrane-Associated Glycans in Developing Zebrafish. *Science (80-.).* **320**, 664–667 (2008).

16. Rossin, R. *et al.* In Vivo Chemistry for Pretargeted Tumor Imaging in Live Mice. *Angew. Chemie Int. Ed.* **49**, 3375–3378 (2010).

17. Yang, J., Šečkutė, J., Cole, C. M. & Devaraj, N. K. Live-Cell Imaging of Cyclopropene Tags with Fluorogenic Tetrazine Cycloadditions. *Angew. Chemie Int. Ed.* **51**, 7476–7479 (2012).

18. Zeglis, B. M. *et al.* A Pretargeted PET Imaging Strategy Based on Bioorthogonal Diels-Alder Click Chemistry. *J. Nucl. Med.* **54**, 1389–1396 (2013).

19. Carlson, J. C. T., Meimetis, L. G., Hilderbrand, S. A. & Weissleder, R. BODIPY-Tetrazine Derivatives as Superbright Bioorthogonal Turn-on Probes. *Angew. Chemie Int. Ed.* **52**, 6917–6920 (2013).

20. Denk, C. *et al.* Design, Synthesis, and Evaluation of a Low-Molecular-Weight 11 C-Labeled Tetrazine for Pretargeted PET Imaging Applying Bioorthogonal in Vivo Click Chemistry. *Bioconjug. Chem.* **27**, 1707–1712 (2016).

21. Vázquez, A. *et al.* Mechanism-Based Fluorogenic trans -Cyclooctene-Tetrazine Cycloaddition. *Angew. Chemie Int. Ed.* **56**, 1334–1337 (2017).

22. Azoulay, M., Tuffin, G., Sallem, W. & Florent, J.-C. A new drug-release method using the Staudinger ligation. *Bioorg. Med. Chem. Lett.* **16**, 3147–3149 (2006).

23. Yusop, R. M., Unciti-Broceta, A., Johansson, E. M. V., Sánchez-Martín, R. M. & Bradley, M. Palladium-mediated intracellular chemistry. *Nat. Chem.* **3**, 239–243 (2011).

24. Matikonda, S. S. *et al.* Bioorthogonal prodrug activation driven by a strain-promoted 1,3-dipolar cycloaddition. *Chem. Sci.* **6**, 1212–1218 (2015).

25. Versteegen, R. M., Rossin, R., ten Hoeve, W., Janssen, H. M. & Robillard, M. S. Click to Release: Instantaneous Doxorubicin Elimination upon Tetrazine Ligation. *Angew. Chemie Int. Ed.* **52**, 14112–14116 (2013).

26. Oliveira, B. L., Guo, Z. & Bernardes, G. J. L. Inverse electron demand Diels–Alder reactions in chemical biology. *Chem. Soc. Rev.* **46**, 4895–4950 (2017).

27. Rossin, R. *et al.* Triggered Drug Release from an Antibody–Drug Conjugate Using Fast “Click-to-Release” Chemistry in Mice. *Bioconjug. Chem.* **27**, 1697–1706 (2016).

28. Mejia Oneto, J. M., Khan, I., Seebald, L. & Royzen, M. In Vivo Bioorthogonal Chemistry Enables Local Hydrogel and Systemic Pro-Drug To Treat Soft Tissue Sarcoma. *ACS Cent. Sci.* **2**, 476–482 (2016).

29. Zhang, G. *et al.* Bioorthogonal chemical activation of kinases in living systems. *ACS Cent. Sci.* **2**, 325–331 (2016).

30. Agustin, E. *et al.* A fast click–slow release strategy towards the HPLC-free synthesis of RNA. *Chem. Commun.* **52**, 1405–1408 (2016).

31. Du, S. *et al.* Cell type-selective imaging and profiling of newly synthesized proteomes by using puromycin analogues. *Chem. Commun.* **53**, 8443–8446 (2017).

32. Carlson, J. C. T., Mikula, H. & Weissleder, R. Unraveling Tetrazine-Triggered Bioorthogonal Elimination Enables Chemical Tools for Ultrafast Release and Universal Cleavage. *J. Am. Chem. Soc.* **140**, 3603–3612 (2018).

33. Sarris, A. J. C. *et al.* Fast and pH-Independent Elimination of trans -Cyclooctene by Using Aminoethyl-Functionalized Tetrazines. *Chem. – A Eur. J.* **24**, 18075–18081 (2018).

34. Versteegen, R. M. *et al.* Click-to-Release from trans -Cyclooctenes: Mechanistic Insights and Expansion of Scope from Established Carbamate to Remarkable Ether Cleavage. *Angew. Chemie Int. Ed.* **57**, 10494–10499 (2018).

35. Rautio, J. *et al.* Prodrugs: design and clinical applications. *Nat. Rev. Drug Discov.* **7**, 255–270 (2008).

36. Rossin, R. *et al.* Chemically triggered drug release from an antibody-drug conjugate leads to potent antitumour activity in mice. *Nat. Commun.* **9**, 1484 (2018).

37. Alouane, A., Labruère, R., Le Saux, T., Schmidt, F. & Jullien, L. Self-Immolative Spacers: Kinetic Aspects, Structure-Property Relationships, and Applications. *Angew. Chemie Int. Ed.* **54**, 7492–7509 (2015).

38. Carl, P. L., Chakravarty, P. K. & Katzenellenbogen, J. A. A novel connector linkage applicable in prodrug design. *J. Med. Chem.* **24**, 479–480 (1981).

39. Kratz, F., Müller, I. A., Ryppa, C. & Warnecke, A. Prodrug Strategies in Anticancer Chemotherapy. *ChemMedChem* **3**, 20–53 (2008).

40. Schuster, H. J. *et al.* Synthesis of the first spacer containing prodrug of a duocarmycin analogue and determination of its biological activity. *Org. Biomol. Chem.* **8**, 1833 (2010).

41. Leu, Y.-L., Chen, C.-S., Wu, Y.-J. & Chern, J.-W. Benzyl Ether-Linked Glucuronide Derivative of 10-Hydroxycamptothecin Designed for Selective Camptothecin-Based Anticancer Therapy. *J. Med. Chem.* **51**, 1740–1746

(2008).

42. Alaoui, A. El, Saha, N., Schmidt, F., Monneret, C. & Florent, J.-C. New Taxol® (paclitaxel) prodrugs designed for ADEPT and PMT strategies in cancer chemotherapy. *Bioorg. Med. Chem.* **14**, 5012–5019 (2006).

43. Kumar, S. K., Williams, S. A., Isaacs, J. T., Denmeade, S. R. & Khan, S. R. Modulating paclitaxel bioavailability for targeting prostate cancer. *Bioorg. Med. Chem.* **15**, 4973–4984 (2007).

44. Satyam, A. Design and synthesis of releasable folate–drug conjugates using a novel heterobifunctional disulfide-containing linker. *Bioorg. Med. Chem. Lett.* **18**, 3196–3199 (2008).

45. Chen, S. *et al.* Mechanism-Based Tumor-Targeting Drug Delivery System. Validation of Efficient Vitamin Receptor-Mediated Endocytosis and Drug Release. *Bioconjug. Chem.* **21**, 979–987 (2010).

46. Burke, P. J. *et al.* Design, Synthesis, and Biological Evaluation of Antibody−Drug Conjugates Comprised of Potent Camptothecin Analogues. *Bioconjug. Chem.* **20**, 1242–1250 (2009).

47. Chakravarty, P. K., Carl, P. L., Weber, M. J. & Katzenellenbogen, J. A. Plasmin-activated prodrugs for cancer chemotherapy. 2. Synthesis and biological activity of peptidyl derivatives of doxorubicin. *J. Med. Chem.* **26**, 638–644 (1983).

48. de Groot, F. M. H., de Bart, A. C. W., Verheijen, J. H. & Scheeren, H. W. Synthesis and Biological Evaluation of Novel Prodrugs of Anthracyclines for Selective Activation by the Tumor-Associated Protease Plasmin. *J. Med. Chem.* **42**, 5277–5283 (1999).

49. Shamis, M. & Shabat, D. Single-Triggered AB6 Self-Immolative Dendritic Amplifiers. *Chem. - A Eur. J.* **13**, 4523–4528 (2007).

50. Lee, H. Y., Jiang, X. & Lee, D. Kinetics of Self-Immolation: Faster Signal Relay over a Longer Linear Distance? *Org. Lett.* **11**, 2065–2068 (2009).

51. Alouane, A. *et al.* Light Activation for the Versatile and Accurate Kinetic Analysis of Disassembly of Self-Immolative Spacers. *Chem. - A Eur. J.* **19**, 11717–11724 (2013).

52. Alouane, A. *et al.* Disassembly Kinetics of Quinone-Methide-Based Self-Immolative Spacers that Contain Aromatic Nitrogen Heterocycles. *Chem. - An Asian J.* **9**, 1334–1340 (2014).

53. Erez, R. & Shabat, D. The azaquinone-methide elimination: comparison study of 1,6- and 1,4-eliminations under physiological conditions. *Org. Biomol. Chem.* **6**, 2669 (2008).

54. Senter, P. D., Pearce, W. E. & Greenfield, R. S. Development of a drug-release strategy based on the reductive fragmentation of benzyl carbamate disulfides. *J. Org. Chem.* **55**, 2975–2978 (1990).

55. de Groot, F. M. H. *et al.* Elongated Multiple Electronic Cascade and Cyclization Spacer Systems in Activatible Anticancer Prodrugs for Enhanced Drug Release. *J. Org. Chem.* **66**, 8815–8830 (2001).

56. Hay, M. P., Sykes, B. M., Denny, W. A. & O'Connor, C. J. Substituent effects on the kinetics of reductively-initiated fragmentation of nitrobenzyl carbamates designed as triggers for bioreductive prodrugs. *J. Chem. Soc. Perkin Trans. 1* 2759–2770 (1999). doi:10.1039/a904067f

57. Robbins, J. S., Schmid, K. M. & Phillips, S. T. Effects of Electronics, Aromaticity, and Solvent Polarity on the Rate of Azaquinone–Methide-Mediated Depolymerization of Aromatic Carbamate Oligomers. *J. Org. Chem.* **78**, 3159–3169 (2013).

58. Mosey, R. A. & Floreancig, P. E. Versatile approach to α-alkoxy carbamate synthesis and stimulus-responsive alcohol release. *Org. Biomol. Chem.* **10**, 7980 (2012).

59. Smith, M. B. & March, J. *March's Advanced Organic Chemistry. Reactions, Mechanisms, and Structure*. (Wiley, 2007).

60. Schmid, K. M., Jensen, L. & Phillips, S. T. A Self-Immolative Spacer That Enables Tunable Controlled Release of Phenols under Neutral Conditions. *J. Org. Chem.* **77**, 4363–4374 (2012).

61. DeWit, M. A. & Gillies, E. R. A Cascade Biodegradable Polymer Based on Alternating Cyclization and Elimination Reactions. *J. Am. Chem. Soc.* **131**, 18327–18334 (2009).

62. DeWit, M. A. & Gillies, E. R. Design, synthesis, and cyclization of 4-aminobutyric acid derivatives: potential candidates as self-immolative spacers. *Org. Biomol. Chem.* **9**, 1846 (2011).

63. Dewit, M. A., Beaton, A. & Gillies, E. R. A reduction sensitive cascade biodegradable linear polymer. *J. Polym. Sci. Part A Polym. Chem.* **48**, 3977–3985 (2010).

64. de Gracia Lux, C. *et al.* Single UV or Near IR Triggering Event Leads to Polymer Degradation into Small Molecules. *ACS Macro Lett.* **1**, 922–926 (2012).

65. Greenwald, R. B. *et al.* Drug Delivery Systems Based on Trimethyl Lock Lactonization: Poly(ethylene glycol) Prodrugs of Amino-Containing Compounds. *J. Med. Chem.* **43**, 475–487 (2000).

66. Grether, U. & Waldmann, H. An Enzyme-Labile Safety Catch Linker for

Synthesis on a Soluble Polymeric Support. *Chemistry (Easton).* **7**, 959–971 (2001).

67. Zheng, A., Shan, D., Shi, X. & Wang, B. A Novel Resin Linker for Solid-Phase Peptide Synthesis Which Can Be Cleaved Using Two Sequential Mild Reactions. *J. Org. Chem.* **64**, 7459–7466 (1999).

68. Levine, M. N. & Raines, R. T. Trimethyl lock: a trigger for molecular release in chemistry, biology, and pharmacology. *Chem. Sci.* **3**, 2412 (2012).

69. Zheng, A., Shan, D. & Wang, B. A Redox-Sensitive Resin Linker for the Solid Phase Synthesis of C- Terminal Modified Peptides. *J. Org. Chem.* **64**, 156–161 (1999).

70. Jung, M. E. & Piizzi, G. gem -Disubstituent Effect: Theoretical Basis and Synthetic Applications. *Chem. Rev.* **105**, 1735–1766 (2005).

71. Wang, D. *et al.* Carboxyl BODIPY Dyes from Bicarboxylic Anhydrides: One-Pot Preparation, Spectral Properties, Photostability, and Biolabeling. *J. Org. Chem.* **74**, 7675–7683 (2009).

72. Dawson, R. M. C., Elliott, D. C., Elliott, W. H. & Jones, K. M. *Data for Biochemical Research*. (Clarendon Press, 1989).

73. Cesar Castro Palomino Laria, Julio; Marti Clauzel, Luc; Zorzano Olarte, Antonio; Garcia Vicente, Silvia; Mian, A. Genmedica Therapeutics SL. Thiocarbonates as anti-inflammatory and antioxidant compounds useful for treating metabolic disorders. US 2012/0149769 A1. Jun 14, 2012.

74. Fomina, N., McFearin, C. L., Sermsakdi, M., Morachis, J. M. & Almutairi, A. Low Power, Biologically Benign NIR Light Triggers Polymer Disassembly. *Macromolecules* **44**, 8590–8597 (2011).

75. Shen, Z., Dornan, P. K., Khan, H. A., Woo, T. K. & Dong, V. M. Mechanistic Insights into the Rhodium-Catalyzed Intramolecular Ketone Hydroacylation. *J. Am. Chem. Soc.* **131**, 1077–1091 (2009).

76. Yoshimura, T., Tomohara, K. & Kawabata, T. Asymmetric Induction via Short-Lived Chiral Enolates with a Chiral C–O Axis. *J. Am. Chem. Soc.* **135**, 7102–7105 (2013).

77. DiLauro, A. M., Seo, W. & Phillips, S. T. Use of Catalytic Fluoride under Neutral Conditions for Cleaving Silicon–Oxygen Bonds. *J. Org. Chem.* **76**, 7352–7358 (2011).

List of Figures

Abbildung 1. Gegenüberstellung der etablierten Click-to-Release Strategie (a) und der erweiterten Strategie für Click-to-Release Experimente mit selbstzerstörenden Linkern (b). 3

Figure 1. Comparison of the established click-to-release strategy (a) and the extended strategy for click-to-release experiments using self-immo-lative linkers (b). 4

Figure 2. Simplified reaction between an allylic functionalized TCO (rTCO) and tetrazine derivatives leading to release of amines from the 1,4-tautomer by cleavage of carbamates: after activation within an inverse-electron-demand Diels-Alder cycloaddition the 4,5-dihydropyridazine is transferred via tautomerization to 1,4-dihydropyridazine releasing an amine upon an electron cascade elimination. 7

Figure 3. Mechanistic insights of the postclick network[32] showing interconversion species and release. The formation of a tricyclic dead-end species is the reason for poor release. Another dead-end caused by oxidation is only formed slowly. Remaining structures are identical to Figure 2. 8

Figure 4. Established tetrazines for click-to-release experiments (selection): literatures standard tetrazine dimethyltetrazine (DMT), mono- (MPA)[32] and bispropanoic acid functionalized tetrazine derivatives (PA_2),[32] aminoethyl functionalized tetrazine derivative (K7.HCl)[33] and bis(pyridine-3-ol) tetrazine derivative $PyrH_2$. 9

Figure 5. Connection setup of a SIL connected to its protecting group (trigger) and the compound of interest (reporter). Upon activation due to an external effector, the protecting moiety is removed leading to an activated species which decomposes spontaneous within several cascade reactions (self-immolation). At the end of the disassembly the active compound (reporter) is obtained. The scheme shows a linkage of two SILs. 10

Figure 6. Schematic representation of a) 1,4-elimination[50–52] and b) 1,6-elimination-based[50,52–54] SILs (drawn without substituents). Upon cleavage of the protecting group reveals its intrinsic nucleophilicity that liberates the desired compound within an electronic cascade reaction in a) ortho- or b) para-delocalization. In case of hydroxy species, a quinone methide intermediate is formed, whereas an azaquinone methide respectively a thiaquinone methide intermediate is the result of amine or thiol species decomposition during the cascade elimination. PG = protecting group; X = O, NH or S; LG = leaving group. 11

Figure 7. Schematic representation of cyclization-based SILs (drawn without substituents). Upon cleavage of the protecting group reveals its intrinsic nucleophilicity that liberates the desired compound within a S_N2t-mediated cyclization. In the case of linker based on a) alkyl

chains,[61–64] heterocycles are obtained as byproducts whereas b) aromatic heterocycles result for ortho substituted aromatic systems.[65–68] PG = protecting group; LG = leaving group. 12

Figure 8. Comparison of the extended strategy for click-to-release experiments using self immolative linkers (left) with the classical click-to-release strategy (right) for the release of carbamates. 15

Figure 9. Structural connection setup to optimize limitations in terms of bioorthogonal compatibility, kinetics and complete release: Usage of carbamates to ensure bioorthogonal compatibility as well as fast release and N-Me substitution of rTCO´s carbamate to provide complete release. The introduction of a PEG chain ensures aqueous kinetic investigations, while the fluorescent dye of a BODIPY[71] derivative allows for quantification. Depending on the nature of the leaving group, the carbamate linking the SIL and the reporter motif is also incorporated in reverse. 16

Figure 10. Target molecule for phenol release experiments: a cyclization-based SIL (red fragment, SIL1) connected to its rTCO protecting group and a phenolic reporter motif. Removal of the rTCO protecting group and subsequent spacer disassembly to a cyclic urea derivative should release the desired phenolic reporter motif as indicated. 17

Figure 11. Target molecule for primary alcohol release experiments: a cyclization-based SIL (red fragment, SIL1) connected to its rTCO protecting group and a primary alcohol reporter motif. Removal of the rTCO protecting group and subsequent spacer disassembly to a cyclic urea derivative should release the desired primary alcohol reporter motif as indicated. 17

Figure 12. Target molecule for primary amine release experiments: a cyclization-based SIL (red fragment, SIL1) connected to its rTCO protecting group and to a further elimination-based SIL (orange fragment, SIL2) containing a primary amine reporter motif located at the end of the self-immolative cascade. Removal of the rTCO protecting group and subsequent spacer disassembly to a cyclic urea derivative as well as a quinone methide intermediate should release the desired primary amine reporter motif as indicated. 18

Figure 13. Synthesis of 1 by HBTU mediated coupling of methyl ester protected *L*-tyrosine and BODIPY-acid. 19

Figure 14. Synthesis of 2 by pNP carbonate activation of 1. 19

Figure 15. One-pot synthesis of 3 by introduction of the cyclization-based SIL1 onto 2. 20

Figure 16. Synthesis of 4 by i) methyl ester deprotection of 3 and ii) HBTU mediated coupling of the free acid and m-PEG7-amine. 21

Figure 17. Synthesis of 5 by HBTU mediated coupling of methyl ester protected *L*-serine and BODIPY-acid. 21

Figure 18. Synthesis of 6 by i) methyl ester deprotection of 5 and ii) HBTU mediated coupling of the free acid and m-PEG7-amine. 22

Figure 19. Synthesis of 7 by i) pNP carbonate activation of 6 and ii) insertion of the cyclization-based SIL1 within a one-pot sequence. 22

Figure 20. Synthesis of 8 by i) methyl ester reduction of a salicyl acid derivative, ii) TBDMS protection of the benzylic hydroxy group and iii) pNP carbonate activation of the phenolic hydroxy group. 23

Figure 21. One-pot synthesis of 9 by introduction of the cyclization-based SIL1 onto 8. 24

Figure 22. Synthesis of 10 by i) TBDMS deprotection of 9 and ii) pNP carbonate activation of the benzylic hydroxy group. 25

Figure 23. One-pot synthesis of 11 by HBTU mediated coupling of N^{ϵ}-Boc protected *L*-lysine, BODIPY-acid and m-PEG7-amine 25

Figure 24. Synthesis of 12 by i) Boc deprotection of 11 and ii) insertion of the rTCO-SIL precursor for release of primary amines (10) onto the deprotected amine intermediate. 26

Figure 25. Proposed self-immolative mechanism for phenol release of a cyclization-based SIL: Upon reaction with tetrazine derivatives used, the initial click adduct leads to the release of an uncaged amine (DMEDA-SIL) via cleavage of carbamates. Subsequently the activated SIL is cleaved after self-immolation, resulting in the release of the final phenolic reporter motif. An oxidized dead-end species was not observed within all kinetic investigations performed. All intermediates contained BODIPY-labeled species 28

Figure 26. BODIPY labeled species distribution of phenol release in CA/P buffer (pH 5, pH 6, pH 7.4 and pH 9 at 37 °C) upon click-to-release and self-immolation mediated by DMT. Quantitative distributions of released fluorophore species were determined from fluorescent chromatograms, which were integrated at 500 nm and normalized to 100 %. 30

Figure 27. Duration of phenol release as a function of pH using DMT as initiator. Whereas only slow release was observed at pH 5 (> 24 h, data not shown), a fundamentally release enhancement at pH 6 (< 24 h, data not shown) was followed by an extensive acceleration of release kinetics within pH 7 to pH 9. A pronounced optimum at pH 9 was identified. PBS at pH 7.4 was similar to CA/P buffer at pH 9. 30

Figure 28. BODIPY labeled species distribution of phenol release in CA/P buffer pH 8 at 37 °C upon click-to-release and self-immolation mediated by MPA, PA_2, K7.HCl and $PyrH_2$. Quantitative distributions of released fluorophore species were determined from fluorescent chromatograms, which were integrated at 500 nm and normalized to 100 %. 31

Figure 29. Proposed self-immolative mechanism for primary alcohol release of a cyclization-based SIL: Upon reaction with tetrazine derivatives used, the initial click adduct leads to the release of an uncaged amine (DMEDA-SIL) via cleavage of carbamates. Subsequently the activated SIL should be cleaved after self-immolation, resulting in the release of the final primary alcohol reporter motif. However, this was not the case. An oxidized dead-end species was not observed within all kinetic investigations performed. All intermediates contained BODIPY-labeled species. 32

Figure 30. Proposed self-immolative mechanism for primary amine release of a combination of cyclization-based (SIL1) and elimination-based (SIL2) SILs: Upon reaction with tetrazine

derivatives used, the initial click adduct leads to the release of an uncaged amine (DMEDA-SIL) via cleavage of carbamates. Subsequently the activated DMEDA-SIL is cleaved after self-immolation, resulting in the release of an activated phenolic-SIL that releases the final amine reporter motif after self-immolation. An oxidized dead-end species was not observed within all kinetic investigations performed. All intermediates contained BODIPY-labeled species. . 33

Figure 31. BODIPY labeled species distribution of primary amine release in CA/P buffer (pH 6, pH 7, pH 7.4 and pH 8 at 37 °C) upon click-to-release and self-immolation mediated by DMT. Quantitative distributions of released fluorophore species were determined from fluorescent chromatograms, which were integrated at 500 nm and normalized to 100 %. Within all kinetic measurements performed, no free phenolic-SIL was observed..... 34

Figure 32. Duration of primary amine release as a function of pH using DMT as initiator. Whereas only slow release was observed at pH 6 (~1 d, data not shown), a fundamentally release enhancement at pH 7 was followed by further acceleration of release kinetics at pH 7.4 and pH 8. A pronounced optimum at pH 8 was identified. 35

Figure 33. BODIPY labeled species distribution of primary amine release in CA/P buffer pH 8 at 37 °C upon click-to-release and self-immolation mediated by MPA, PA_2, K7.HCl and $PyrH_2$. Quantitative distributions of released fluorophore species were determined from fluorescent chromatograms, which were integrated at 500 nm and normalized to 100 %. Within all kinetic measurements performed, no free phenolic-SIL was observed..... 36

Figure 34. Fluorescent chromatogram of BODIPY labeled phenol release species in CA/P buffer pH 6 at 37 °C upon click-to-release and self-immolation (1 h 26 min 51 s after addition of DMT). Several BODIPY species could not be assigned to expected disassembly cascade species (t_R=2.25-2.50 min). 44

Figure 35. Fluorescent chromatogram of BODIPY labeled phenol release species in CA/P buffer pH 7 at 37 °C upon click-to-release and self-immolation (59 min 20 s after addition of DMT). Several BODIPY species could not be assigned to expected disassembly cascade species (t_R=2.25-2.50 min). 45

Figure 36. Fluorescent chromatogram of BODIPY labeled phenol release species in CA/P buffer pH 7 at 37 °C upon click-to-release and self-immolation (2 h 30 min 19 s after addition of DMT). Several BODIPY species could not be assigned to expected disassembly cascade species (t_R=2.25-2.50 min). 45